Published in final edited form as:
Semin Nucl Med. 2012 September ; 42(5): 328–342. doi:10.1053/j.semnuclmed.2012.04.004.

Functional Imaging for Prostate Cancer: Therapeutic Implications

Carina Mari Aparici, MD[1,2] and **Youngho Seo, PhD**[1,3,4]

[1]Department of Radiology and Biomedical Imaging, University of California, San Francisco, CA.

[2]Nuclear Medicine Service, San Francisco Veterans Affairs Medical Center, San Francisco, CA.

[3]Department of Radiation Oncology, Helen Diller Family Comprehensive Cancer Center, University of California San Francisco, CA.

[4]UC Berkeley-UCSF Graduate Program in Bioengineering, University of California, San Francisco, CA.

Abstract

Functional radionuclide imaging modalities, now commonly combined with anatomical imaging modalities CT or MRI (SPECT/CT, PET/CT, and PET/MRI) are promising tools for the management of prostate cancer particularly for therapeutic implications. Sensitive detection capability of prostate cancer using these imaging modalities is one issue; however, the treatment of prostate cancer using the information that can be obtained from functional radionuclide imaging techniques is another challenging area. There are not many SPECT or PET radiotracers that can cover the full spectrum of the management of prostate cancer from initial detection, to staging, prognosis predictor, and all the way to treatment response assessment. However, when used appropriately, the information from functional radionuclide imaging improves, and sometimes significantly changes, the whole course of the cancer management. The limitations of using SPECT and PET radiotracers with regards to therapeutic implications are not so much different from their limitations solely for the task of detecting prostate cancer; however, the specific imaging target and how this target is reliably imaged by SPECT and PET can potentially make significant impact in the treatment of prostate cancer. Finally, while the localized prostate cancer is considered manageable, there is still significant need for improvement in noninvasive imaging of metastatic prostate cancer, in treatment guidance, and in response assessment from functional imaging including radionuclide-based techniques. In this review article, we present the rationale of using functional radionuclide imaging and the therapeutic implications for each of radionuclide imaging agent that have been studied in human subjects.

Introduction

Prostate cancer is the most common noncutaneous malignancy among men in the United States, and rated second in mortality after lung cancer, accounting for estimated 9.3% of all cancer-related deaths of male adults (28,170 out of 301,820) in 2012.[1] This disease is age-related, therefore, as life expectancy increases, so will its incidence, creating a significant health problem.[2] The successful management of prostate cancer requires early detection of clinically significant disease, appropriate risk assessment, and optimum treatment.[3,4] Digital rectal examination (DRE)[5] is considered the standard reference for detection of prostate cancer with 50% of all palpable nodules being carcinomas. Prostate cancer is currently

Address for Mailing Proofs: Youngho Seo, PhD, UCSF Physics Research Laboratory, 185 Berry Street, Suite 350, San Francisco, CA 94107 Telephone Number: +1-415-353-9464 for Youngho Seo, PhD Fax Number: +1-415-353-9421 youngho.seo@ucsf.edu.

characterized by its prostate-specific antigen (PSA) serum level, TNM stage, and Gleason score.[6] The PSA testing is useful for screening prostate cancer, and has been a good marker for assessing response to therapy and detecting recurrent and/or metastatic disease. It is believed to have reduced the rate of death from prostate cancer, but the PSA lacks the ability to differentiate low-grade from high-grade cancers, and there remains a growing concern regarding the potential risk of overdiagnosis and, consequently, overtreatment of potentially indolent disease based on PSA levels, affecting the quality of life of patients in this group.[4]

The treatments of prostate cancer include radical prostatectomy (RP), pelvic lymph node dissection (PLND), external beam radiotherapy (EBRT), brachytherapy, cryosurgery, hyperthermia, androgen deprivation therapy (ADT), and chemotherapy. Monotherapy or combination therapy is performed based on the staging and clinical presentation of the cancer. Among the available treatment options, definitive treatments, meaning eradicating or killing the cancer tissues, include RP that often combines with PLND or extended PLND (ePLND),[7-12] EBRT that often combines with prophylactic pelvic irradiation,[13-18] and brachytherapy.[19-28] Since the definitive treatments are inevitably invasive, which could lead to unwanted, significant side effects, understanding of tumor boundaries and spread prior to the treatments has become a significant healthcare challenge. The pretherapy assessment for these definitive therapeutic approaches involves conventional noninvasive radiologic imaging such as transrectal ultrasound (TRUS), x-ray computed tomography (CT), magnetic resonance imaging (MR), and radionuclide bone scintigraphy (bone scan).[29] However, for these definitive treatments, identifying disease versus nondisease volumes is difficult using any of the available imaging methods.

Functional imaging proves its value in these therapeutic implications by providing information on the biologically active volume of the cancer. The currently performed functional or metabolic imaging techniques for prostate cancer evaluations are radionuclide imaging techniques such as single photon emission computed tomography (SPECT) and positron emission tomography (PET) as well as magnetic resonance imaging (MRI) techniques that provide functional and metabolic information of the cancer such as dynamic contrast-enhanced (DCE) MRI[30,31], ultrasmall superparamagnetic iron oxide (USPIO)-MRI,[32,33] proton high-resolution magic angle spinning (HR-MAS) magnetic resonance spectroscopic imaging (MRSI),[34-37] or hyperpolarized ^{13}C-pyruvate metabolic MRI.[38,39] All of these functional imaging techniques have limited utilities in prostate cancer management; as no single imaging modality provides reliable methods of delineating cancerous lesions clearly from nondisease volumes, which has become a significant challenge of using noninvasive imaging results in definitive therapies of prostate cancer.

Fortunately, these advanced imaging modalities, combined with current imaging technologies, provide more direct means of being utilized in treatment planning than before because either radionuclide-based or metabolic/spectroscopic MR-based information is accompanied by structural imaging information such as CT[40-42] and conventional MRI.[35,37,43,44] The structural imaging information locates functional and metabolic signals in relation to the patient anatomy; thus help delineate or identify the volumes of biological significance for therapeutic inventions. In this report, the focus is given to radionuclide-based imaging techniques using modern SPECT/CT and PET/CT technologies, and how the functional radionuclide imaging information can be used in therapeutic interventions will be discussed in detail.

The sections that follow will describe presently studied molecular imaging radiotracers that are used in clinical prostate cancer imaging, and how the CT and MRI complement the functional information from the radionuclide imaging as mediators. The roles of functional

prostate cancer imaging in guiding therapies, drug or radiation therapy response monitoring, the assessment of recurrent or residual disease after definitive treatments will be discussed.

Combined Radionuclide and Structural Imaging Modalities for Prostate Cancer Management

Examining the extent of prostate cancer spread, once PSA and DRE provides enough suspicion followed by cancer presence confirmed by TRUS-guided biopsies, noninvasive imaging, regardless of its being functional or structural, can potentially provide the information on how spread the cancer is. Although this may be true in most other cancers to some degree, noninvasive imaging has not fulfilled its promise to provide accurate information with regards to the involvement of prostate cancer (*i.e.*, status of regional, distant, and bone metastasis). In terms of functional radionuclide imaging technologies, the advent of combined dual-modality SPECT/CT, PET/CT, and PET/MRI for clinical applications has not progressed much for the detection and diagnosis of prostate cancer. However, the structural imaging techniques from CT and MRI in the combined dual-modality scanners are still very useful if there is any complementary anatomical information that can help the therapeutic management of the prostate cancer.

SPECT/CT

SPECT/CT is currently offered as SPECT scanners combined with either low-mA CT or high-mA CT as in standalone CT scanners from major vendors.[40,45] The utility of CT in SPECT image reconstruction has been found to be significant so that SPECT images have greatly improved by having CT-based information such as attenuation map.[40,46,47] The primary difference between low-mA CT and high-mA CT is how CT is used in relation to localization of radiotracer uptake patterns from SPECT.[48] The high-mA CT offers conspicuity of anatomical references. In cancer evaluations using the radionuclide imaging techniques that do not provide clear anatomical features, high-mA CT offers more than simply providing attenuation map for SPECT reconstruction as shown in Fig. 1. For the prostate cancer, the radiation treatment or surgical guidance during PLND can benefit from the combined SPECT/CT technologies.[49,50] Although the low specificity is problematic, the common radiotracers used in gamma camera and SPECT imaging, such as ^{99m}Tc-(hydroxyl)methylene diphosphonate (HDP or MDP), ^{99m}Tc-labeled colloidal particles (albumin colloid or sulfur colloid), ^{111}In-capromab pendetide (ProstaScint), all provide useful information in guiding customized therapy planning. The details of each tracer's role, in conjunction with SPECT/CT scanners, will be provided in separate sections below.

PET/CT

PET with ^{18}F-fluorodeoxyglucose (FDG), now more commonly as combined dual-modality PET/CT, changed the cancer management scheme significantly in recent years.[51-55] FDG has become a very important radiotracer that connects the glucose utilization and tumor growth.[56,57] In prostate cancer evaluation, its utility still is questionable as a general imaging technique for staging; however, ^{18}F-FDG can be used for the assessment of distant metastasis.[58,59] Bone scan with PET using ^{18}F-NaF[60-65] as an imaging tracer is increasingly used in those geographical regions where a nearby radiopharmacy can provide ^{18}F-NaF to PET centers, as is the case for ^{18}F-FDG. For prostate cancer in general, the increasing use of PET/CT, for which the combined CT provides powerful structural information and direct therapy planning guidance, is predictable since there are already several PET imaging radiotracers other than ^{18}F-FDG that showed a promising clinical utility such as ^{11}C/^{18}F-choline[66-85] (an example image is shown in Fig. 2), ^{11}C/^{18}F-acetate,[69,75,86-98] and ^{18}F-fluorodihydrotestosterone (FDHT).[99-101] Some of these PET radiotracers have good potential to guide treatment planning and monitor treatment response.

PET/MRI

PET/MRI, an emerging field of active research investigations, is still finding its utility in clinical applications.[102-105] In potential clinical applications using PET/MRI, the importance of MRI in relation to PET may be more significant than CT to PET/CT particularly considering the MRI's excellent soft tissue contrast; thus the design of PET/MRI scanners does emphasize the performance of MRI as well as that of PET while they are put together either simultaneously or side-by-side. MR-specific techniques that have been developed for prostate cancer imaging can further benefit from PET radiopharmaceuticals that have found utilities in prostate cancer evaluation. In an ideal situation, PET/MRI could make a significant impact for prostate cancer management because the combined imaging techniques offer superior structural/functional/metabolic information *in vivo* than any other combinations of imaging modalities currently available in the clinical setting. However, a routine practice of using PET/MRI still needs to be defined for the prostate cancer management, which is a nontrivial question. One strong potential using PET/MRI for prostate cancer is that this combined scanner can be one-stop shopping for new drug therapy response assessment in patients, which can be applied to many cancer types. Also, when there is a strong need of performing both MR-based techniques and PET studies for patients with prostate cancer, the combined PET/MRI scanner could save some time for patients avoiding two separate visits. Most of MR techniques that are useful in prostate cancer detection and evaluation, such as DCE-MRI, USPIO-MRI, MRSI, and hyperpolarized ^{13}C-pyruvate MRI, can be implemented in PET/MRI without significant compromise, while the increasingly popular efforts of PET imaging agent developments targeting specific biomarkers of prostate cancer such as prostate-specific membrane antigen (PSMA)[106-109] and prostate stem cell antigen (PSCA)[110] will be able to strongly complement the MR-based findings as well. However, the question of using simultaneous PET/MRI will always be subject to controversies while both PET and MRI imaging information can be obtained without any compromise from separate scanners with optimized settings for each.

Therapeutic Approaches and Radionuclide Imaging for Prostate Cancer Management

In the US, National Comprehensive Cancer Network (NCCN) publishes guidelines for standardized cancer managements including prostate cancer.[111-116] The NCCN prostate cancer clinical practice guideline provides up-to-date management flow charts that contain both imaging and therapeutic approaches. The use of noninvasive imaging in the NCCN guideline is limited to the standard imaging techniques such as abdominal-pelvic CT/MRI and bone scan because, while limited for prostate cancer evaluation, these two imaging techniques are widely available. Considering that according to the NCCN guidelines in therapy planning, the imaging techniques are used for evaluating the lymphatic and bony involvement, it can be also directly implied that the imaging techniques that can provide sensitive measures of bone and lymph node involvement have great potential to be adopted in the clinical practice guidelines. It should be noted that one of the most extensively studied radionuclide imaging agents, ^{111}In-ProstaScint, has been removed in the most current NCCN guideline as a recommended method in the recurrent setting of the prostate cancer, indicating the frustration of not having a reliable and highly sensitive functional imaging agent.

Since the functional imaging methods are being adopted as drug therapy response monitoring for most types of cancer, nonspecific but sensitive lymph node and bone imaging methods such as ultrasmall superparamagnetic iron oxide (USPIO)-MRI and bone SPECT and PET are being considered in clinical research settings. Androgen deprivation therapy (ADT), chemotherapy (when ADT is ineffective for castration-resistant prostate cancer

(CRPC)), and bisphosphonates therapy (for bone mineral density (BMD) improvement in case of bone metastasis[117-125]), can potentially benefit from functional imaging-based sensitive lymph node and bone involvement assessment techniques as well.

Radionuclide Imaging Agents for Prostate Cancer

There are a number of radionuclide-based imaging agents that were developed and are under development in laboratory research settings for prostate cancer.[126-128] However, if we focus on radionuclide-based imaging agents and techniques that have been made to extensive clinical evaluations in conjunction with therapeutic implications, the list of radiotracers becomes relatively short-handed.

Bone-Seeking Agents – ^{99m}Tc-MDP/HDP, ^{18}F-NaF

The rationale of bone imaging for prostate cancer is that the metastasis to bones can typically change the whole course of the cancer management because of its indication of the advanced stage. Thus, the bone metastasis evaluation is important when the systemic treatment approach such as ADT and chemotherapy is considered for advanced prostate cancer patients. Bone-seeking agents using radionuclides accumulate in the lesions where increased blood flow and osteoblastic activity exist in bone. In the case of bone metastasis, this accumulation shows a typical random pattern of conspicuous osteoblastic lesions mainly along the axial and proximal appendicular skeleton. Although not specific for bone metastases of only prostate cancer, radionuclide bone scans have proven to be very useful in the assessment of bone metastases.

Sentinel Lymph Node (SLN) Involvement Agents – ^{99m}Tc-albumin colloid, ^{99m}Tc-sulfur colloid

Even after definitive treatments, patients without clear evidence of metastatic disease, relapse at a very high rate.[17,129] From PLND and ePLND studies performed, the lymph node involvement of prostate cancer seems higher than typically thought.[130] As a treatment method, PLND can benefit greatly if it targets identified SLNs or lymph nodes within the lymphatic path drainage of the prostate.[130-143] As shown in the literature, the location of prostate sentinel lymph nodes and lymph node drainage varies significantly between patients.[50,144] In addition, as a prophylactic measure, pelvic lymph node irradiation for intermediate-to-high risk patients should be more reliably designed when the identification of sentinel and/or drainage lymph nodes is made before the irradiation.[49] Functional radionuclide imaging helps in this regard. For both surgeries and radiation therapy, the SLN imaging can be adopted as a routine evaluation before the treatments.

Prostate-Specific Membrane Antigen (PSMA)- Targeting Agents – ^{111}In-capromab pendetide (ProstaScint), ^{177}Lu-J591 (for radioimmunotherapy, but imaging can be performed), ^{123}I-MIP-1072

Prostate-specific membrane antigen (PSMA) is overexpressed in malignant prostate tissue,[145] and has been pursued as a preferred target for prostate cancer imaging as well as therapy as targeted radionuclide therapy. PSMA is known to be expressed in some normal cells, and when the cancer becomes metastatic to bones, the expression of PSMA is significantly diminished as undetectable PSMA levels are found in PC-3 cells that are derived from prostate cancer bone metastasis. In malignant lymph nodes, PSMA is highly expressed as in LNCaP cells, which has been confirmed by $^{\text{in vivo}}$ imaging experiments.[107,146] For this reason, PSMA is considered an excellent target for prostate cancer evaluation particularly of lymph node involvement, but may not be preferred as a single imaging target to cover bone metastasis of the prostate cancer. The monoclonal murine antibody, targeting the intracellular epitope of PSMA, 7E11-C5 had progressed to a

clinical product for imaging when labeled with In-111 (^{111}In-ProstaScint). Although the promise of anti-PSMA imaging may have diminished significantly because of the low sensitivity and specificity of ^{111}In-ProstaScint, there has been still extensive research studies using PSMA as a target of prostate cancer imaging and therapy.

Non-prostate-specific Metabolic PET Imaging Agents – ^{18}F-fluorodeoxyglucose (FDG), ^{11}C/^{18}F-choline, ^{11}C/^{18}F-acetate

PET and PET/CT imaging of ^{18}F-fluorodeoxyglucose (FDG) to visualize the tumor glucose utilization has become the gold standard for staging most cancers. Not specifically effective in prostate cancer, FDG still finds its utility in this malignancy in terms of evaluating distant metastasis when there is a risk defined by other parameters such as PSA and Gleason score from biopsies. Metabolic PET imaging agents for the investigations of glucose, choline, and acetate metabolism have been studied in patients with prostate cancer.

Androgen Receptor and Protein Synthesis Imaging Agents – ^{18}F-fluorodihydrotestosterone (FDHT), ^{11}C-methionine

Since androgen deprivation therapy is common to suppress growth of prostate cancer systemically, imaging androgen receptor is a natural step to follow that therapy. ^{18}F-FDHT has been developed to follow the level of androgen receptor expression, and has been correlated with anti-androgen treatment of prostate cancer.[101,126,147]

Protein synthesis and amino acid transport in tumor proliferation can be followed by radiolabeled amino acid such as ^{11}C-methionine.[126] However, the role of ^{11}C-methionine is still limited to detection of prostate cancer, and its therapeutic implications are still understudied.

Radionuclide Imaging of Prostate Cancer and Therapeutic Implications

In the following, we describe the underlying mechanism of each radionuclide imaging agent and its therapeutic implications followed by representative examples. Our manuscript is not intended to compile all available and studied radionuclide imaging agents that have shown their values in imaging prostate cancer. There are several review articles for that topic already, and this review article is focused on the radionuclide imaging of prostate cancer and their therapeutic implications.

Bone Imaging and Therapy

Bone scan, whether it is performed using SPECT (^{99m}Tc-MDP/HDP) or PET (^{18}F-NaF) is a standard imaging method to visualize turnover anomalies in the bone. In prostate cancer, whole-body bone scan is used as a monitor for progression of metastatic bone disease.

^{99m}Tc-phosphonate tracers such as MDP and HDP are absorbed to bone matrix where calcium phosphate exchanges with phosphonate compounds. The higher exchange or turnover rate means the higher osteoblastic activity, which presented in a specific pattern is a good indication of metastasis. ^{18}F-NaF is also rapidly absorbed to bone matrix, and the uptake of fluoride ion of ^{18}F-NaF shows anomalies associated with bone metabolic disorders including prostate cancer bone metastasis. Using two-dimensional anterior-posterior bone scan, SPECT, SPECT/CT, PET, or PET/CT, the bone metabolism can be tracked, and for the therapeutic implications, the radionuclide imaging of bone metabolism is an excellent resource to allow cancer progression monitoring or therapy response evaluation and monitoring.

For example, the bone scan findings were correlated as a prognostic factor of survival and a stratification tool in clinical trials of drug therapy of bone metastasis.[148,149] When outcomes and predictive factors for biochemical relapse were measured for patients without bone metastasis, the patient stratification could be made with negative radionuclide bone scan.[150] The lesion volume of bone involvement of prostate cancer assessed by bone scan has proven to be a strong prognostic value. In patients with primary androgen deprivation therapy (ADT), the site of bone metastasis identified by bone scan was also found to carry a good prognostic value of survival.[151] Bone scan findings could be directly compared before and after ADT, showing the geographically inconsistent response to the therapy in bone lesions (as shown in Fig. 3), the value of noninvasive bone imaging to assess the treatment response for the metastatic prostate cancer.[152]

The limitation of bone scan for prostate bone metastasis evaluation using any radionuclide imaging modality and agent currently available still lies within the lack of cancer-specificity of the agent. It is a major challenge to develop an imaging probe specific for metastatic prostate cancer that can reliably investigate the effect of direct cancer therapeutics targeting bone metastasis of the prostate cancer.

Sentinel Lymph Node (SLN) Imaging and Therapy

Radionuclide sentinel lymph node imaging using SPECT(/CT) or intraoperative gamma camera could make a significant contribution in both surgical and radiation interventions of prostate cancer. Both PLND and ePLND during radical prostatectomy, and pelvic irradiation during external beam radiotherapy, can target identified sentinel lymph nodes and/or lymph nodes along the prostate's lymphatic drainage more aggressively, or avoid nonsentinel nodes if the removal or irradiation of them could cause nonnegligible side effects.

The patient-specific lymphatic drainage pattern identification from the prostate gland has been possible using radionuclide-based colloidal particles. For example, Fig. 4 shows the distribution of multiple lymph nodes within the lymphatic drainage of the prostate identified by radionuclide colloidal particle imaging.[153] Earlier attempts of radionuclide imaging ^{99m}Tc-labeled colloid (e.g., ^{99m}Tc-antimony sulphide colloid[154]) showed its feasibility of noninvasive imaging of SLN distribution from the prostate. Nanocolloids (colloidal particles with the size less than 100 nm) have preferential accumulation at the first landing sites, also known as sentinel lymph nodes (SLNs), through the lymphatic drainage chain as for all other colloidal particle; however because of their small sizes, the drainage from the administered site to lymph nodes is faster than larger colloids so that the imaging window is within a few hours after administration. When labeled with radionuclides such as Tc-99m and because of the size of nanocolloids, the clearance from the prostate gland and accumulation time in the lymph nodes do not require hours of wait time before imaging studies. Commercial products like ^{99m}Tc-Nanocoll (GE Healthcare), nanocolloid of human serum albumin,[144,153,155] which is not available in the United States, and ^{99m}Tc-sulfur nanocolloid (filtered through a 100-nm polycarbonate membrane filter) can be easily administered to the prostate gland under the guidance of TRUS.[49]

In surgical procedures of radical prostatectomy and PLND, ^{99m}Tc-nanocolloid images from either preoperative SPECT registered onto CT or MRI, or intraoperative gamma probe showed guiding resections of SLNs reliably.[156] From the data review from the surgical cases, SLN imaging techniques supported that PLND for prostate cancer should be extensive, including common iliac nodes up to the utreteric crossing.[155]

In radiation treatment using intensity-modulated ratiotherapy (IMRT) for prostate cancer, when the individual lymphatic drainage map from radionuclide nanocolloid imaging is available, it is found to be feasible to selectively irradiate SLNs and other lymph nodes

within the particular lymphatic drainage of that prostate that could be missed by CT-based planning only.[144,157] The implication of this approach is that the pelvic lymph node irradiation based on individualized lymphatic drainage of the prostate could increase the curative potential of radiotherapy in high-risk patients who have a higher probability of lymph node involvement of the cancer. In addition, the study performed in the USA using ^{99m}Tc-sulfur nanocolloid showed a similar potential of the radionuclide SLN imaging in guiding IMRT planning and whole-pelvis radiotherapy (WPRT).[158] In this study, there were clear cases of substantially altered radiation fields based on the SLN imaging results.

The limitation of the radionuclide SLN imaging includes that this imaging technique is only reliably applicable for the patients who have the intact prostate that has not been treated because of the uncertainty of where the radioactive nanocolloids can be administered. Additional limitation is the lack of the long-term effect data from the altered, if any, treatment management of the prostate cancer, either surgical or radiation interventions. Hence, once the radionuclide SLN imaging is more adopted in routine clinical practice, there will be more definitive data to show the actual benefit from the therapeutic approaches based on the radionuclide SLN imaging.

Anti-PSMA Imaging and Therapy

PSMA is the most well-established imaging target of prostate cancer because of its overexpression in malignant prostate cancer.[159-162] Radionuclide imaging against PSMA using monoclonal antibody (mAb) also has been extensively performed both in clinical settings and small animal models of prostate cancer. The clinical anti-PSMA radionuclide imaging is performed using ^{111}In-capromab pendetide (ProstaScint), which is the only PSMA-targeting imaging agent currently approved by the US Food and Drug Administration (FDA).[163,164] The imaging information from ^{111}In-ProstaScint has been utilized in the therapeutic approaches of prostate cancer. However, the success of the clinical impact on the therapeutic management of the cancer is rather controversial.

Two other radionuclide imaging agents targeting PSMA have been studied in the phased clinical trials. The first is radiolabeled J591 mAb which targets the extracellular epitope of PSMA.[165-170] Unlike ^{111}In-ProstaScint with its antibody (7E11-C5) targeting the intracellular epitope of PSMA, ^{111}In-J591 has been considered a superior imaging agent for anti-PSMA imaging.[165] However, the current effort of using J591 mAb is toward its use in targeted radionuclide therapy (radioimmunotherapy) labeled with a therapeutic radionuclide, Lu-177 and Y-90.[170-173] By its own targeting specificity, this approach is also promising to be therapeutically effective on prostate cancer cells that express high levels of PSMA. And, the more recent effort of using J591 is to combine with a positron-emitting radionuclide, Zr-89 via a bifunctional chelate desferrioxamine B (DFO), making ^{89}Zr-DFO-J591 for immunoPET imaging of prostate cancer.[99,174] The second radionuclide imaging agent targeting PSMA, which has been also studied in human subjects is ^{123}I-MIP-1072,[175] developed by Molecular Insight Pharmaceuticals (Cambridge, MA). ^{123}I-MIP-1072 is a small molecule (535 Da), glutamate-urea heterodimer inhibiting the N-acetylated α-linked acidic dipeptidase (NAALADase) enzymatic activity of PSMA, and preferentially accumulates and internalizes in cells expressing PSMA. This imaging agent has been pursued in human subjects as a couple of Phase I clinical trials which were completed in between 2009 and 2011.

The PSMA-targeting radionuclide imaging agents, thus, have a great potential of therapy planning, particularly for the lymph node involvement of the prostate cancer or for the heterogeneity of the cancer, subject to the localized brachytherapy. For example, ^{111}In-ProstaScint SPECT/CT was able to make feasible dose escalation to the biological target volumes (BTVs) identified by the imaging for brachytherapy (as shown in Fig. 5).[21,176] This

feasibility study was also supported by the SPECT/CT studies of ^{111}In-ProstaScint for the patients presented with clinically localized cancer, which found that the biochemical failure from radiotherapy was higher for the group of patients who had extra-periprostatic metastasis versus the group of patients who had confined localized cancer by the ^{111}In-ProstaScint SPECT/CT findings.[177] Although it is still controversial and not generally accepted, the prognostic value of quantitative ^{111}In-ProstaScint SPECT/CT imaging findings could be highly relevant and correlative with the cancer prognostic factor such as pathologic Gleason score.[178] The prognostic value of this imaging study will likely be strengthened when a more robust PSMA-targeting radionuclide imaging agent can be used in human subjects. Hence, imaging agents such as ^{89}Zr-DFO-J591, ^{123}I-MIP-1072, or any other emerging PSMA-targeting radionuclide imaging agent, have generally a great potential to help therapy guidance, while providing a prognostic value.

Non-prostate-specific Metabolic PET Imaging and Therapy

The use of FDG-PET/CT in the cancer management has greatly impacted on the patient welfare for many cancer types. Although its utility in prostate cancer detection is relatively low, FDG-PET/CT provides still very relevant information to stage the prostate cancer when the distant lymph node involvement is suspected. FDG PET/CT has shown that disseminated and aggressive lymph node metastasis of the prostate cancer can be visualized.[71,179] In terms of therapeutic interventions, the finding of disseminated lymph node metastasis can be significant, and response to either ADT or chemotherapy can be monitored when there are lesions identified by this imaging modality. Other cancer nonspecific, but still metabolically cancer-avid radionuclide imaging agents have been used in PET imaging of prostate cancer. For this reason, the metabolic activity of prostate cancer can be used in relation to the treatment management. The metabolism of prostate cancer that can be assessed by PET includes glucose (^{18}F-FDG), acetate (^{11}C-acetate and ^{18}F-fluoroacetate), and choline (^{11}C-choline, ^{18}F-fluorocholine, and ^{18}F-fluoroethylcholine). Although these metabolic PET imaging agents except ^{18}F-FDG are not generally available, the synthesis of these radiotracers are well published, and the availability depends on the dedicated onsite or regional radiopharmacy facilities for PET imaging centers.

It has been understood that primary prostate cancer cells display limited expression of GLUT-1 transporters, resulting in low accumulation of ^{18}F-FDG in tumor sites.[180] The tumor generally is characterized by increased choline metabolism in the cell to meet increased phosphatidylcholine synthesis, an important element of cell membrane phospholipids.[85]^{11}C-choline PET for imaging recurrent prostate cancer and its metastases has been used for this reason.[91] Prostate epithelial cells undergo a metabolic transition from citrate-producing normal cells to citrate-oxidizing malignant cells.[181] This alteration in citrate metabolism in prostate epithelial cells also leads to an increased turnover of acetate. This prostate-specific citrate metabolism may contribute to high radiopharmaceutical uptake of ^{11}C-acetate, and several studies have shown that ^{11}C-acetate has marked uptake in prostate cancer and its metastasis.[93,94,96,97] In comparison to ^{18}F-FDG, ^{11}C-acetate PET studies showed higher accuracies for pelvic lymph node metastases.[87,93]

At a clinical practice where a PET/CT scanner exists without an onsite cyclotron, ^{18}F-labeled versions of choline or acetate (^{18}F-fluoroacetate,[182,183]^{18}F-fluorocholine,[141,184-190] and ^{18}F-fluoroethylcholine[191-195]) is presumably an alternative;[182] however the clinical use of ^{18}F-labeled choline or acetate is somewhat inconsistent with the results from the studies using ^{11}C-labeled choline or acetate because of the difference in pharmacokinetics.

Although FDG is not routinely used for prostate cancer evaluation, when there is uptake identified in patients with prostate cancer by FDG, the lesion and FDG uptake can be followed for the treatment. For example, the relationship between the effect of androgen

ablation and the glucose utilization (by FDG uptake measures) has been studied.[196] In this study, there was some indication of FDG uptake affected by the treatment decrease in the lesion identified before and after androgen ablation. Brachytherapy or any focal therapy such as hyperthermia[197] does not benefit greatly from FDG because of the usual high uptake of FDG found in bladder obscuring the visualization and quantification of FDG uptake in the nearby organs including the prostate.

In case of ^{11}C- or ^{18}F-labeled choline, because of its wider availability or interest than other ^{11}C- or ^{18}F-labeled nonFDG PET radiotracers for prostate cancer, it has been considered to use the lesions identified by choline-PET in radiation treatment planning[198] or surgical interventions such as RP and PLND. Although it is still hard to recommend as a routine clinical practice, some very promising results were reported recently about using ^{11}C-choline PET/CT to guide lymph node dissections while radical prostatectomy was performed in patients.[199] In this study, 3 out of 6 patients with single lymph node metastasis identified by ^{11}C-choline showed a complete permanent PSA remission without adjuvant therapy for approximately 2 years of follow-up. A further study from the same authors, using both ^{11}C-choline and ^{18}F-fluoroethylcholine, showed a similar result that reported 4 out of 9 patients with single lymph node metastasis had a complete permanent PSA remission for approximately 2.5 years of follow-up.[200] In these investigations, one example PET/CT image showing a single lymph node metastasis identified by ^{11}C-choline is illustrated in Fig. 6.

In case of ^{11}C- or ^{18}F-labeled acetate, the same principle of its choline counterparts can be applied in terms of its therapeutic implications. PET imaging using radiolabeled choline, acetate, and FDG all detect lymph nodes and even bone metastasis when its corresponding metabolism is avid in these lesions. A dual-isotope study using ^{11}C-acetate and ^{18}F-FDG showed that the detected bone lesions by both imaging agents were affected by androgen deprivation therapy.[201] It is not surprising to find out this result because the tumors that depend on glucose utilization or acetate metabolism should be affected by the systemic ADT. In radiation treatment planning, it is natural to believe that the information from ^{11}C/^{18}F-acetate PET can be included for possible boost of radiation to the biological target volume (BTV). A theoretical study has shown that it is indeed feasible[202], but the validation study of using ^{11}C-acetate (or even ^{18}F-acetate or ^{11}C/^{18}F-choline compounds) still needs to be performed to be widely accepted.

A significant limitation of using metabolic PET imaging agents for therapy planning or therapy response assessment is that none of these imaging agents is cancer specific. Because of this reason, both choline and acetate-based PET imaging agents also showed a high rate of false-negative findings.[203,204] In addition, since there are also too many trials and errors to find this general tumor imaging agent in case that FDG fails to reliably deliver a good diagnosis, there is no focused effort of pursuing a limited set of imaging agents and careful investigations are hard to achieve.

Androgen Receptor Imaging and Therapy

Another ^{18}F-labeled PET imaging agent, ^{18}F-fluorodihydrotestosterone (FDHT) targets androgen receptors, and has been evaluated for imaging prostate cancer. Dihydrotestosterone (DHT) is directly correlated with the expression of androgen receptor[100,205] that has a major role in tumor growth even in castration-resistant prostate cancer (CRPC). As an imaging agent, ^{18}F-FDHT may not be superior to other metabolic PET imaging agents mentioned earlier; however, since ^{18}F-FDHT is correlated with the androgen reception expression, it is a promising imaging agent to show the effect of anti-androgen therapy of prostate cancer as shown in Fig. 7. However, only limited studies have

been performed to correlate ADT and ^{18}F-FDHT uptake changes in advanced prostate tumors.[100,147]

Imaging Agents Under Development and Therapeutic Implications

There are a number of radionuclide-based imaging agents that were developed and are under development in research settings for prostate cancer. It should be again clearly noted that his paper is not intended to compile the list of imaging agents that still need extensive research before clinical translation. For that topic, there are some recent excellent review articles published.[99,126,127,206]

The management of clinical localized prostate cancer has improved significantly in recent years with the survival rates being very high, much of the attention is paid to identifying and systemically treating disseminated disease. For example, the imaging target such as PSMA is actively pursued also for therapeutic target of radioimmunotherapy.[146,171,172] In addition, there is much interest in using anti-PSMA antibodies or small molecules as a vehicle for the drug payload. For the PSMA-targeted systemic therapy, the role of radionuclide imaging using the same vehicle could be significant as a tool for patient stratification. The same principle of imaging and therapy can be applied to any other antibodies[110,207] or small molecules[106,107,109] that target PSMA or other antigens specific to prostate cancer.

Acknowledgments

This work was supported by grants K25 CA114254 from the National Institutes of Health (NIH); K25 CA114254-04S1 American Recovery and Reinvestment Act (ARRA) of 2009 through NIH; and from UCSF Research Evaluation and Allocation Committee and UCSF Department of Radiation Oncology.

References

1. Siegel R, Naishadham D, Jemal A. Cancer statistics, 2012. CA Cancer J Clin. 2012; 62:10–29. [PubMed: 22237781]
2. Cho D, Di Blasio CJ, Rhee AC, et al. Prognostic factors for survival in patients with hormone-refractory prostate cancer (HRPC) after initial androgen deprivation therapy (ADT). Urol Oncol. 2003; 21:282–291. [PubMed: 12954499]
3. Han M, Partin AW, Piantadosi S, et al. Era specific biochemical recurrence-free survival following radical prostatectomy for clinically localized prostate cancer. J Urol. 2001; 166:416–419. [PubMed: 11458039]
4. Stamey TA, Caldwell M, McNeal JE, et al. The prostate specific antigen era in the United States is over for prostate cancer: what happened in the last 20 years? J Urol. 2004; 172:1297–301. [PubMed: 15371827]
5. Hammerer P, Huland H, Sparenberg A. Digital rectal examination, imaging, and systematic-sextant biopsy in identifying operable lymph node-negative prostatic carcinoma. Eur Urol. 1992; 22:281–7. [PubMed: 1283372]
6. Gleason DF. Histologic grading of prostate cancer: a perspective. Hum Pathol. 1992; 23:273–9. [PubMed: 1555838]
7. Briganti A, Karakiewicz PI, Chun FK, et al. Percentage of positive biopsy cores can improve the ability to predict lymph node invasion in patients undergoing radical prostatectomy and extended pelvic lymph node dissection. Eur Urol. 2007; 51:1573–81. [PubMed: 17293026]
8. Touijer K, Rabbani F, Otero JR, et al. Standard versus limited pelvic lymph node dissection for prostate cancer in patients with a predicted probability of nodal metastasis greater than 1%. J Urol. 2007; 178:120–4. [PubMed: 17499306]
9. Allaf ME, Palapattu GS, Trock BJ, et al. Anatomical extent of lymph node dissection: impact on men with clinically localized prostate cancer. J Urol. 2004; 172:1840–4. [PubMed: 15540734]

10. Briganti A, Suardi N, Capogrosso P, et al. Lymphatic spread of nodal metastases in high-risk prostate cancer: The ascending pathway from the pelvis to the retroperitoneum. Prostate. 2012; 72:186–92. [PubMed: 21538428]
11. Briganti A, Chun FK, Salonia A, et al. Critical assessment of ideal nodal yield at pelvic lymphadenectomy to accurately diagnose prostate cancer nodal metastasis in patients undergoing radical retropubic prostatectomy. Urology. 2007; 69:147–51. [PubMed: 17270638]
12. Burkhard FC, Studer UE. The role of lymphadenectomy in high risk prostate cancer. World J Urol. 2008; 26:231–6. [PubMed: 18369636]
13. Seaward SA, Weinberg V, Lewis P, et al. Identification of a high-risk clinically localized prostate cancer subgroup receiving maximum benefit from whole-pelvic irradiation. Cancer J Sci Am. 1998; 4:370–7. [PubMed: 9853136]
14. Seaward SA, Weinberg V, Lewis P, et al. Improved freedom from PSA failure with whole pelvic irradiation for high-risk prostate cancer. Int J Radiat Oncol Biol Phys. 1998; 42:1055–62. [PubMed: 9869229]
15. Asbell SO, Krall JM, Pilepich MV, et al. Elective pelvic irradiation in stage A2, B carcinoma of the prostate: analysis of RTOG 77-06. Int J Radiat Oncol Biol Phys. 1988; 15:1307–16. [PubMed: 3058656]
16. Shih HA, Harisinghani M, Zietman AL, et al. Mapping of nodal disease in locally advanced prostate cancer: rethinking the clinical target volume for pelvic nodal irradiation based on vascular rather than bony anatomy. Int J Radiat Oncol Biol Phys. 2005; 63:1262–9. [PubMed: 16253781]
17. Roach M 3rd, DeSilvio M, Valicenti R, et al. Whole-pelvis, “mini-pelvis,” or prostate-only external beam radiotherapy after neoadjuvant and concurrent hormonal therapy in patients treated in the Radiation Therapy Oncology Group 9413 trial. Int J Radiat Oncol Biol Phys. 2006; 66:647–53. [PubMed: 17011443]
18. Wang-Chesebro A, Xia P, Coleman J, et al. Intensity-modulated radiotherapy improves lymph node coverage and dose to critical structures compared with three-dimensional conformal radiation therapy in clinically localized prostate cancer. Int J Radiat Oncol Biol Phys. 2006; 66:654–62. [PubMed: 17011444]
19. Deutsch I, Zelefsky MJ, Zhang Z, et al. Comparison of PSA relapse-free survival in patients treated with ultra-high-dose IMRT versus combination HDR brachytherapy and IMRT. Brachytherapy. 2011; 9:313–8. [PubMed: 20685176]
20. Ellis RJ, Zhou H, Kaminsky DA, et al. Rectal morbidity after permanent prostate brachytherapy with dose escalation to biologic target volumes identified by SPECT/CT fusion. Brachytherapy. 2007; 6:149–56. [PubMed: 17434109]
21. Ellis RJ, Zhou H, Kim EY, et al. Biochemical disease-free survival rates following definitive low-dose-rate prostate brachytherapy with dose escalation to biologic target volumes identified with SPECT/CT capromab pendetide. Brachytherapy. 2007; 6:16–25. [PubMed: 17284381]
22. Ghadjar P, Rentsch CA, Isaak B, et al. Urethral toxicity vs. cancer control-Lessons to be learned from high-dose rate brachytherapy combined with intensity-modulated radiation therapy in intermediate- and high-risk prostate cancer. Brachytherapy. 2011; 10:286–94. [PubMed: 21030318]
23. Hsu IC, Cabrera AR, Weinberg V, et al. Combined modality treatment with high-dose-rate brachytherapy boost for locally advanced prostate cancer. Brachytherapy. 2005; 4:202–6. [PubMed: 16182220]
24. King CR. LDR vs. HDR brachytherapy for localized prostate cancer: the view from radiobiological models. Brachytherapy. 2002; 1:219–226. [PubMed: 15062170]
25. Hsu IC, Pickett B, Shinohara K, et al. Normal tissue dosimetric comparison between HDR prostate implant boost and conformal external beam radiotherapy boost: potential for dose escalation. Int J Radiat Oncol Biol Phys. 2000; 46:851–8. [PubMed: 10705005]
26. Pouliot J, Kim Y, Lessard E, et al. Inverse planning for HDR prostate brachytherapy used to boost dominant intraprostatic lesions defined by magnetic resonance spectroscopy imaging. Int J Radiat Oncol Biol Phys. 2004; 59:1196–207. [PubMed: 15234056]

27. Ghadjar P, Matzinger O, Isaak B, et al. Association of urethral toxicity with dose exposure in combined high-dose-rate brachytherapy and intensity-modulated radiation therapy in intermediate- and high-risk prostate cancer. Radiother Oncol. 2009; 91:237–42. [PubMed: 19167121]
28. Eng TY, Thomas CR, Herman TS. Primary radiation therapy for localized prostate cancer. Urol Oncol. 2002; 7:239–57. [PubMed: 12504845]
29. Hricak H, Choyke PL, Eberhardt SC, et al. Imaging prostate cancer: a multidisciplinary perspective. Radiology. 2007; 243:28–53. [PubMed: 17392247]
30. van Lin EN, Futterer JJ, Heijmink SW, et al. IMRT boost dose planning on dominant intraprostatic lesions: gold marker-based three-dimensional fusion of CT with dynamic contrast-enhanced and 1H-spectroscopic MRI. Int J Radiat Oncol Biol Phys. 2006; 65:291–303. [PubMed: 16618584]
31. Noworolski SM, Henry RG, Vigneron DB, et al. Dynamic contrast-enhanced MRI in normal and abnormal prostate tissues as defined by biopsy, MRI, and 3D MRSI. Magn Reson Med. 2005; 53:249–55. [PubMed: 15678552]
32. Barentsz JO, Futterer JJ, Takahashi S. Use of ultrasmall superparamagnetic iron oxide in lymph node MR imaging in prostate cancer patients. Eur J Radiol. 2007; 63:369–72. [PubMed: 17689215]
33. Harisinghani MG, Saksena MA, Hahn PF, et al. Ferumoxtran-10-enhanced MR lymphangiography: does contrast-enhanced imaging alone suffice for accurate lymph node characterization? AJR Am J Roentgenol. 2006; 186:144–8. [PubMed: 16357394]
34. Lian J, Hunjan S, Dumoulin C, et al. Integrating deformable MRI/MRSI and CT image registration into the prostate IMRT treatment planning. Int J Radiat Oncol Biol Phys. 2003; 57:S207.
35. Kurhanewicz J, Swanson MG, Nelson SJ, et al. Combined magnetic resonance imaging and spectroscopic imaging approach to molecular imaging of prostate cancer. J Magn Reson Imaging. 2002; 16:451–463. [PubMed: 12353259]
36. Mueller-Lisse UG, Swanson MG, Vigneron DB, et al. Time-dependent effects of hormone-deprivation therapy on prostate metabolism as detected by combined magnetic resonance imaging and 3D magnetic resonance spectroscopic imaging. Magn Reson Med. 2001; 46:49–57. [PubMed: 11443710]
37. Swanson MG, Vigneron DB, Tran TK, et al. Magnetic resonance imaging and spectroscopic imaging of prostate cancer. Cancer Invest. 2001; 19:510–523. [PubMed: 11458818]
38. Brindle KM, Bohndiek SE, Gallagher FA, et al. Tumor imaging using hyperpolarized 13C magnetic resonance spectroscopy. Magn Reson Med. 2011; 66:505–19. [PubMed: 21661043]
39. Kurhanewicz J, Vigneron DB, Brindle K, et al. Analysis of cancer metabolism by imaging hyperpolarized nuclei: prospects for translation to clinical research. Neoplasia. 2011; 13:81–97. [PubMed: 21403835]
40. Seo Y, Mari C, Hasegawa BH. Technological development and advances in single-photon emission computed tomography/computed tomography. Semin Nucl Med. 2008; 38:177–98. [PubMed: 18396178]
41. Cherry SR. Multimodality imaging: beyond PET/CT and SPECT/CT. Semin Nucl Med. 2009; 39:348–53. [PubMed: 19646559]
42. Bockisch A, Freudenberg LS, Schmidt D, et al. Hybrid imaging by SPECT/CT and PET/CT: proven outcomes in cancer imaging. Semin Nucl Med. 2009; 39:276–89. [PubMed: 19497404]
43. Coakley FV, Qayyum A, Kurhanewicz J. Magnetic resonance imaging and spectroscopic imaging of prostate cancer. J Urol. 2003; 170:S69–75. discussion S75-6. [PubMed: 14610414]
44. Kurhanewicz J, Swanson MG, Wood PJ, et al. Magnetic resonance imaging and spectroscopic imaging: Improved patient selection and potential for metabolic intermediate endpoints in prostate cancer chemoprevention trials. Urology. 2001; 57:124–8. [PubMed: 11295609]
45. Mariani G, Bruselli L, Kuwert T, et al. A review on the clinical uses of SPECT/CT. Eur J Nucl Med Mol Imaging. 2010; 37:1959–85. [PubMed: 20182712]
46. Hasegawa BH, Wong KH, Iwata K, et al. Dual-modality imaging of cancer with SPECT/CT. Technol Cancer Res Treat. 2002; 1:449–58. [PubMed: 12625772]
47. Seo Y, Wong KH, Sun M, et al. Correction of photon attenuation and collimator response for a body-contouring SPECT/CT imaging system. J Nucl Med. 2005; 46:868–77. [PubMed: 15872362]

48. Aparici CM, Carlson D, Nguyen N, et al. Combined SPECT and Multidetector CT for Prostate Cancer Evaluations. Am J Nucl Med Mol Imaging. 2012; 2:48–54. [PubMed: 22267999]
49. Seo Y, Aparici CM, Chen CP, et al. Mapping of lymphatic drainage from the prostate using filtered 99mTc-sulfur nanocolloid and SPECT/CT. J Nucl Med. 2011; 52:1068–72. [PubMed: 21680690]
50. Warncke SH, Mattei A, Fuechsel FG, et al. Detection rate and operating time required for gamma probe-guided sentinel lymph node resection after injection of technetium-99m nanocolloid into the prostate with and without preoperative imaging. Eur Urol. 2007; 52:126–32. [PubMed: 17258385]
51. Saif MW, Tzannou I, Makrilia N, et al. Role and cost effectiveness of PET/CT in management of patients with cancer. Yale J Biol Med. 2010; 83:53–65. [PubMed: 20589185]
52. Otsuka H, Morita N, Yamashita K, et al. FDG-PET/CT for cancer management. J Med Invest. 2007; 54:195–9. [PubMed: 17878667]
53. Czernin J, Schelbert HR. PET/CT in cancer patient management. Introduction. J Nucl Med. 2007; 48(Suppl 1):2S–3S.
54. Endo K, Oriuchi N, Higuchi T, et al. PET and PET/CT using 18F-FDG in the diagnosis and management of cancer patients. Int J Clin Oncol. 2006; 11:286–96. [PubMed: 16937302]
55. Bar-Shalom R, Yefremov N, Guralnik L, et al. Clinical performance of PET/CT in evaluation of cancer: additional value for diagnostic imaging and patient management. J Nucl Med. 2003; 44:1200–9. [PubMed: 12902408]
56. Buck AK, Herrmann K, Shen C, et al. Molecular imaging of proliferation in vivo: positron emission tomography with [18F]fluorothymidine. Methods. 2009; 48:205–15. [PubMed: 19318128]
57. Ott K, Herrmann K, Schuster T, et al. Molecular imaging of proliferation and glucose utilization: utility for monitoring response and prognosis after neoadjuvant therapy in locally advanced gastric cancer. Ann Surg Oncol. 2011; 18:3316–23. [PubMed: 21537865]
58. Schoder H, Larson SM. Positron emission tomography for prostate, bladder, and renal cancer. Semin Nucl Med. 2004; 34:274–92. [PubMed: 15493005]
59. Fricke E, Machtens S, Hofmann M, et al. Positron emission tomography with 11C-acetate and 18F-FDG in prostate cancer patients. Eur J Nucl Med Mol Imaging. 2003; 30:607–11. [PubMed: 12589476]
60. Cook GJ, Parker C, Chua S, et al. 18F-fluoride PET: changes in uptake as a method to assess response in bone metastases from castrate-resistant prostate cancer patients treated with 223Ra-chloride (Alpharadin). EJNMMI Res. 2011; 1:4. [PubMed: 22214491]
61. Langsteger W, Balogova S, Huchet V, et al. Fluorocholine (18F) and sodium fluoride (18F) PET/CT in the detection of prostate cancer: prospective comparison of diagnostic performance determined by masked reading. Q J Nucl Med Mol Imaging. 2011; 55:448–57. [PubMed: 21738117]
62. Beheshti M, Langsteger W, Fogelman I. Prostate cancer: role of SPECT and PET in imaging bone metastases. Semin Nucl Med. 2009; 39:396–407. [PubMed: 19801219]
63. Beheshti M, Vali R, Waldenberger P, et al. Detection of bone metastases in patients with prostate cancer by 18F fluorocholine and 18F fluoride PET-CT: a comparative study. Eur J Nucl Med Mol Imaging. 2008; 35:1766–74. [PubMed: 18465129]
64. Hsu WK, Virk MS, Feeley BT, et al. Characterization of osteolytic, osteoblastic, and mixed lesions in a prostate cancer mouse model using 18F-FDG and 18F-fluoride PET/CT. J Nucl Med. 2008; 49:414–21. [PubMed: 18287261]
65. Even-Sapir E, Metser U, Mishani E, et al. The detection of bone metastases in patients with high-risk prostate cancer: 99mTc-MDP Planar bone scintigraphy, single- and multi-field-of-view SPECT, 18F-fluoride PET, and 18F-fluoride PET/CT. J Nucl Med. 2006; 47:287–97. [PubMed: 16455635]
66. Picchio M, Spinapolice EG, Fallanca F, et al. [11C]choline PET/CT detection of bone metastases in patients with PSA progression after primary treatment for prostate cancer: comparison with bone scintigraphy. Eur J Nucl Med Mol Imaging. 2012; 39:13–26. [PubMed: 21932120]
67. Giovacchini G. Do we have to withdraw antiandrogenic therapy in prostate cancer patients before PET/CT with [11C]choline? Eur J Nucl Med Mol Imaging. 2011; 38:1964–6. [PubMed: 21901380]

68. Fuccio C, Schiavina R, Castellucci P, et al. Androgen deprivation therapy influences the uptake of 11C-choline in patients with recurrent prostate cancer: the preliminary results of a sequential PET/CT study. Eur J Nucl Med Mol Imaging. 2011; 38:1985–9. [PubMed: 21732105]
69. Jambor I, Borra R, Kemppainen J, et al. Functional imaging of localized prostate cancer aggressiveness using 11C-acetate PET/CT and 1H-MR spectroscopy. J Nucl Med. 2010; 51:1676–83. [PubMed: 20956477]
70. Piert M, Park H, Khan A, et al. Detection of aggressive primary prostate cancer with 11C-choline PET/CT using multimodality fusion techniques. J Nucl Med. 2009; 50:1585–93. [PubMed: 19759109]
71. Richter JA, Rodriguez M, Rioja J, et al. Dual tracer 11C-choline and FDG-PET in the diagnosis of biochemical prostate cancer relapse after radical treatment. Mol Imaging Biol. 2010; 12:210–7. [PubMed: 19543774]
72. Picchio M, Crivellaro C, Giovacchini G, et al. PET-CT for treatment planning in prostate cancer. Q J Nucl Med Mol Imaging. 2009; 53:245–68. [PubMed: 19293771]
73. Krause BJ, Souvatzoglou M, Tuncel M, et al. The detection rate of [11C]choline-PET/CT depends on the serum PSA-value in patients with biochemical recurrence of prostate cancer. Eur J Nucl Med Mol Imaging. 2008; 35:18–23. [PubMed: 17891394]
74. Reske SN, Blumstein NM, Glatting G. [11C]choline PET/CT imaging in occult local relapse of prostate cancer after radical prostatectomy. Eur J Nucl Med Mol Imaging. 2008; 35:9–17. [PubMed: 17828534]
75. Nanni C, Castellucci P, Farsad M, et al. 11C/ 18F-choline PET or 11C/18F-acetate PET in prostate cancer: may a choice be recommended? Eur J Nucl Med Mol Imaging. 2007; 34:1704–5. [PubMed: 17619877]
76. Scher B, Seitz M, Albinger W, et al. Value of 11C-choline PET and PET/CT in patients with suspected prostate cancer. Eur J Nucl Med Mol Imaging. 2007; 34:45–53. [PubMed: 16932935]
77. Martorana G, Schiavina R, Corti B, et al. 11C-choline positron emission tomography/computerized tomography for tumor localization of primary prostate cancer in comparison with 12-core biopsy. J Urol. 2006; 176:954–60. discussion 960. [PubMed: 16890665]
78. Reske SN, Blumstein NM, Neumaier B, et al. Imaging prostate cancer with 11C-choline PET/CT. J Nucl Med. 2006; 47:1249–54. [PubMed: 16883001]
79. Yoshida S, Nakagomi K, Goto S, et al. 11C-choline positron emission tomography in prostate cancer: primary staging and recurrent site staging. Urol Int. 2005; 74:214–20. [PubMed: 15812206]
80. de Jong IJ, Pruim J, Elsinga PH, et al. 11C-choline positron emission tomography for the evaluation after treatment of localized prostate cancer. Eur Urol. 2003; 44:32–8. discussion 38-9. [PubMed: 12814672]
81. Picchio M, Messa C, Landoni C, et al. Value of [11C]choline-positron emission tomography for re-staging prostate cancer: a comparison with [18F]fluorodeoxyglucose-positron emission tomography. J Urol. 2003; 169:1337–40. [PubMed: 12629355]
82. de Jong IJ, Pruim J, Elsinga PH, et al. Preoperative staging of pelvic lymph nodes in prostate cancer by 11C-choline PET. J Nucl Med. 2003; 44:331–5. [PubMed: 12620996]
83. Picchio M, Landoni C, Messa C, et al. Positive [11C]choline and negative [18F]FDG with positron emission tomography in recurrence of prostate cancer. AJR Am J Roentgenol. 2002; 179:482–4. [PubMed: 12130458]
84. de Jong IJ, Pruim J, Elsinga PH, et al. Visualization of prostate cancer with 11C-choline positron emission tomography. Eur Urol. 2002; 42:18–23. [PubMed: 12121724]
85. Hara T, Kosaka N, Kishi H. PET imaging of prostate cancer using carbon-11-choline. J Nucl Med. 1998; 39:990–5. [PubMed: 9627331]
86. Dimitrakopoulou-Strauss A, Strauss LG. PET imaging of prostate cancer with 11C-acetate. J Nucl Med. 2003; 44:556–8. [PubMed: 12679399]
87. Fricke E, Machtens S, Hofmann M, et al. Positron emission tomography with 11C-acetate and 18F-FDG in prostate cancer patients. Eur J Nucl Med Mol Imaging. 2003; 30:607–11. [PubMed: 12589476]

88. Froehner M, Beuthien-Baumann B, Wirth MP. 11C-acetate positron emission tomography for occult prostate cancer. Urol Oncol. 2006; 24:410–1. [PubMed: 16962491]

89. Jadvar H. Prostate cancer: PET with 18F-FDG, 18F- or 11C-acetate, and 18F- or 11C-choline. J Nucl Med. 2011; 52:81–9. [PubMed: 21149473]

90. Kato T, Tsukamoto E, Kuge Y, et al. Accumulation of [11C]acetate in normal prostate and benign prostatic hyperplasia: comparison with prostate cancer. Eur J Nucl Med Mol Imaging. 2002; 29:1492–5. [PubMed: 12397469]

91. Kotzerke J, Volkmer BG, Neumaier B, et al. Carbon-11 acetate positron emission tomography can detect local recurrence of prostate cancer. Eur J Nucl Med Mol Imaging. 2002; 29:1380–4. [PubMed: 12271422]

92. Mena E, Turkbey B, Mani H, et al. 11C-Acetate PET/CT in Localized Prostate Cancer: A Study with MRI and Histopathologic Correlation. J Nucl Med. 2012

93. Oyama N, Akino H, Kanamaru H, et al. 11C-acetate PET imaging of prostate cancer. J Nucl Med. 2002; 43:181–6. [PubMed: 11850482]

94. Oyama N, Miller TR, Dehdashti F, et al. 11C-acetate PET imaging of prostate cancer: detection of recurrent disease at PSA relapse. J Nucl Med. 2003; 44:549–55. [PubMed: 12679398]

95. Schiepers C, Hoh CK, Nuyts J, et al. 1-11C-acetate kinetics of prostate cancer. J Nucl Med. 2008; 49:206–15. [PubMed: 18199613]

96. Soloviev D, Fini A, Chierichetti F, et al. PET imaging with 11C-acetate in prostate cancer: a biochemical, radiochemical and clinical perspective. Eur J Nucl Med Mol Imaging. 2008; 35:942–9. [PubMed: 18338167]

97. Vavere AL, Kridel SJ, Wheeler FB, et al. 1-11C-acetate as a PET radiopharmaceutical for imaging fatty acid synthase expression in prostate cancer. J Nucl Med. 2008; 49:327–34. [PubMed: 18199615]

98. Wachter S, Tomek S, Kurtaran A, et al. 11C-acetate positron emission tomography imaging and image fusion with computed tomography and magnetic resonance imaging in patients with recurrent prostate cancer. J Clin Oncol. 2006; 24:2513–9. [PubMed: 16636343]

99. Rice SL, Roney CA, Daumar P, et al. The next generation of positron emission tomography radiopharmaceuticals in oncology. Semin Nucl Med. 2011; 41:265–82. [PubMed: 21624561]

100. Larson SM, Morris M, Gunther I, et al. Tumor localization of 16beta-18F-fluoro-5alpha-dihydrotestosterone versus 18F-FDG in patients with progressive, metastatic prostate cancer. J Nucl Med. 2004; 45:366–73. [PubMed: 15001675]

101. Zanzonico PB, Finn R, Pentlow KS, et al. PET-based radiation dosimetry in man of 18F-fluorodihydrotestosterone, a new radiotracer for imaging prostate cancer. J Nucl Med. 2004; 45:1966–71. [PubMed: 15534070]

102. Zaidi H, Del Guerra A. An outlook on future design of hybrid PET/MRI systems. Med Phys. 2011; 38:5667–89. [PubMed: 21992383]

103. Pichler BJ, Kolb A, Nagele T, et al. PET/MRI: paving the way for the next generation of clinical multimodality imaging applications. J Nucl Med. 2010; 51:333–6. [PubMed: 20150252]

104. Fatemi-Ardekani A, Samavati N, Tang J, et al. Advances in multimodality imaging through a hybrid PET/MRI system. Crit Rev Biomed Eng. 2009; 37:495–515. [PubMed: 20565381]

105. Delso G, Ziegler S. PET/MRI system design. Eur J Nucl Med Mol Imaging. 2009; 36(Suppl 1):S86–92. [PubMed: 19104809]

106. Banerjee SR, Pullambhatla M, Byun Y, et al. 68Ga-labeled inhibitors of prostate-specific membrane antigen (PSMA) for imaging prostate cancer. J Med Chem. 2010; 53:5333–41. [PubMed: 20568777]

107. Lapi SE, Wahnishe H, Pham D, et al. Assessment of an 18F-labeled phosphoramidate peptidomimetic as a new prostate-specific membrane antigen-targeted imaging agent for prostate cancer. J Nucl Med. 2009; 50:2042–8. [PubMed: 19910433]

108. Elsasser-Beile U, Reischl G, Wiehr S, et al. PET imaging of prostate cancer xenografts with a highly specific antibody against the prostate-specific membrane antigen. J Nucl Med. 2009; 50:606–11. [PubMed: 19289418]

109. Chen Y, Foss CA, Byun Y, et al. Radiohalogenated prostate-specific membrane antigen (PSMA)-based ureas as imaging agents for prostate cancer. J Med Chem. 2008; 51:7933–43. [PubMed: 19053825]
110. Lepin EJ, Leyton JV, Zhou Y, et al. An affinity matured minibody for PET imaging of prostate stem cell antigen (PSCA)-expressing tumors. Eur J Nucl Med Mol Imaging. 2010; 37:1529–38. [PubMed: 20354850]
111. Abdollah F, Schmitges J, Sun M, et al. A population-based assessment of the National Comprehensive Cancer Network practice guideline indications for pelvic lymph node dissection at radical prostatectomy. BJU Int. 2011
112. Poonacha TK, Go RS. Level of scientific evidence underlying recommendations arising from the National Comprehensive Cancer Network clinical practice guidelines. J Clin Oncol. 2011; 29:186–91. [PubMed: 21149653]
113. Crawford ED. Use of algorithms as determinants for individual patient decision making: national comprehensive cancer network versus artificial neural networks. Urology. 2003; 62:13–9. [PubMed: 14706504]
114. Cella D, Paul D, Yount S, et al. What are the most important symptom targets when treating advanced cancer? A survey of providers in the National Comprehensive Cancer Network (NCCN). Cancer Invest. 2003; 21:526–35. [PubMed: 14533442]
115. Scherr D, Swindle PW, Scardino PT. National Comprehensive Cancer Network guidelines for the management of prostate cancer. Urology. 2003; 61:14–24. [PubMed: 12667883]
116. Baker LH, Hanks G, Gershenson D, et al. NCCN Prostate Cancer Practice Guidelines. The National Comprehensive Cancer Network. Oncology (Williston Park). 1996; 10:265–88. [PubMed: 8953609]
117. Fizazi K, Bosserman L, Gao G, et al. Denosumab treatment of prostate cancer with bone metastases and increased urine N-telopeptide levels after therapy with intravenous bisphosphonates: results of a randomized phase II trial. J Urol. 2009; 182:509–15. discussion 515-6. [PubMed: 19524963]
118. Smith MR. Osteoclast targeted therapy for prostate cancer: bisphosphonates and beyond. Urol Oncol. 2008; 26:420–5. [PubMed: 18593621]
119. Polascik TJ. Bone health in prostate cancer patients receiving androgen-deprivation therapy: the role of bisphosphonates. Prostate Cancer Prostatic Dis. 2008; 11:13–9. [PubMed: 17923854]
120. Luftner D, Henschke P, Possinger K. Clinical value of bisphosphonates in cancer therapy. Anticancer Res. 2007; 27:1759–68. [PubMed: 17649770]
121. Gilbert SM, McKiernan JM. The role of bisphosphonates in preventing skeletal complications of hormonal therapy. Urol Clin North Am. 2006; 33:191–9. vi. [PubMed: 16631457]
122. Smith MR. The role of bisphosphonates in men with prostate cancer receiving androgen deprivation therapy. Oncology (Williston Park). 2004; 18:21–5. [PubMed: 15202584]
123. Hoskin PJ. Bisphosphonates and radiation therapy for palliation of metastatic bone disease. Cancer Treat Rev. 2003; 29:321–7. [PubMed: 12927572]
124. Smith MR. Bisphosphonates to prevent osteoporosis in men receiving androgen deprivation therapy for prostate cancer. Drugs Aging. 2003; 20:175–83. [PubMed: 12578398]
125. Paterson AH. The potential role of bisphosphonates as adjuvant therapy in the prevention of bone metastases. Cancer. 2000; 88:3038–46. [PubMed: 10898349]
126. Lutje S, Boerman OC, van Rij CM, et al. Prospects in radionuclide imaging of prostate cancer. Prostate. 2011
127. Beer AJ, Eiber M, Souvatzoglou M, et al. Radionuclide and hybrid imaging of recurrent prostate cancer. Lancet Oncol. 2011; 12:181–91. [PubMed: 20599424]
128. Mease RC. Radionuclide based imaging of prostate cancer. Curr Top Med Chem. 2010; 10:1600–16. [PubMed: 20583988]
129. Spiotto MT, Hancock SL, King CR. Radiotherapy after prostatectomy: improved biochemical relapse-free survival with whole pelvic compared with prostate bed only for high-risk patients. Int J Radiat Oncol Biol Phys. 2007; 69:54–61. [PubMed: 17459606]
130. Weckermann D, Dorn R, Trefz M, et al. Sentinel lymph node dissection for prostate cancer: experience with more than 1,000 patients. J Urol. 2007; 177:916–20. [PubMed: 17296375]

131. Meinhardt W, van der Poel HG, Valdes Olmos RA, et al. Laparoscopic sentinel lymph node biopsy for prostate cancer: the relevance of locations outside the extended dissection area. Prostate Cancer. 2012; 2012:751753. [PubMed: 22111006]

132. Rousseau C, Rousseau T, Bridji B, et al. Laparoscopic sentinel lymph node (SLN) versus extensive pelvic dissection for clinically localized prostate carcinoma. Eur J Nucl Med Mol Imaging. 2012; 39:291–9. [PubMed: 22086144]

133. Schilling D, Boekeler U, Gakis G, et al. Modified concept for radioisotope-guided sentinel lymph node dissection in prostate cancer. World J Urol. 2010; 28:715–20. [PubMed: 20349074]

134. Holl G, Dorn R, Wengenmair H, et al. Validation of sentinel lymph node dissection in prostate cancer: experience in more than 2,000 patients. Eur J Nucl Med Mol Imaging. 2009; 36:1377–82. [PubMed: 19430782]

135. Bastide C, Brenot-Rossi I, Garcia S, et al. Radioisotope guided sentinel lymph node dissection in patients with localized prostate cancer: results of the first 100 cases. Eur J Surg Oncol. 2009; 35:751–6. [PubMed: 18538526]

136. Meinhardt W, Valdes Olmos RA, van der Poel HG, et al. Laparoscopic sentinel node dissection for prostate carcinoma: technical and anatomical observations. BJU Int. 2008; 102:714–7. [PubMed: 18410427]

137. Janetschek G. Can sentinel pelvic lymph node dissection replace extended pelvic lymph node dissection in patients with prostate cancer? Nat Clin Pract Urol. 2007; 4:636–7. [PubMed: 17925808]

138. Brenot-Rossi I, Rossi D, Esterni B, et al. Radioguided sentinel lymph node dissection in patients with localised prostate carcinoma: influence of the dose of radiolabelled colloid to avoid failure of the procedure. Eur J Nucl Med Mol Imaging. 2008; 35:32–8. [PubMed: 17828535]

139. Jeschke S, Beri A, Grull M, et al. Laparoscopic radioisotope-guided sentinel lymph node dissection in staging of prostate cancer. Eur Urol. 2008; 53:126–32. [PubMed: 17434672]

140. Beri A, Janetschek G. Technology insight: radioguided sentinel lymph node dissection in the staging of prostate cancer. Nat Clin Pract Urol. 2006; 3:602–10. [PubMed: 17088928]

141. Hacker A, Jeschke S, Leeb K, et al. Detection of pelvic lymph node metastases in patients with clinically localized prostate cancer: comparison of [18F]fluorocholine positron emission tomography-computerized tomography and laparoscopic radioisotope guided sentinel lymph node dissection. J Urol. 2006; 176:2014–8. discussion 2018-9. [PubMed: 17070241]

142. Corvin S, Schilling D, Eichhorn K, et al. Laparoscopic sentinel lymph node dissection--a novel technique for the staging of prostate cancer. Eur Urol. 2006; 49:280–5. [PubMed: 16364536]

143. Jeschke S, Nambirajan T, Leeb K, et al. Detection of early lymph node metastases in prostate cancer by laparoscopic radioisotope guided sentinel lymph node dissection. J Urol. 2005; 173:1943–6. [PubMed: 15879787]

144. Ganswindt U, Paulsen F, Corvin S, et al. Optimized coverage of high-risk adjuvant lymph node areas in prostate cancer using a sentinel node-based, intensity-modulated radiation therapy technique. Int J Radiat Oncol Biol Phys. 2007; 67:347–55. [PubMed: 17236960]

145. Silver DA, Pellicer I, Fair WR, et al. Prostate-specific membrane antigen expression in normal and malignant human tissues. Clin Cancer Res. 1997; 3:81–5. [PubMed: 9815541]

146. Pan MH, Gao DW, Feng J, et al. Biodistributions of 177Lu- and 111In-labeled 7E11 antibodies to prostate-specific membrane antigen in xenograft model of prostate cancer and potential use of 111In-7E11 as a pre-therapeutic agent for 177Lu-7E11 radioimmunotherapy. Mol Imaging Biol. 2009; 11:159–66. [PubMed: 19034582]

147. Dehdashti F, Picus J, Michalski JM, et al. Positron tomographic assessment of androgen receptors in prostatic carcinoma. Eur J Nucl Med Mol Imaging. 2005; 32:344–50. [PubMed: 15726353]

148. Meirelles GS, Schoder H, Ravizzini GC, et al. Prognostic value of baseline [18F] fluorodeoxyglucose positron emission tomography and 99mTc-MDP bone scan in progressing metastatic prostate cancer. Clin Cancer Res. 2010; 16:6093–9. [PubMed: 20975102]

149. Sabbatini P, Larson SM, Kremer A, et al. Prognostic significance of extent of disease in bone in patients with androgen-independent prostate cancer. J Clin Oncol. 1999; 17:948–57. [PubMed: 10071289]

150. Hori S, Jabbar T, Kachroo N, et al. Outcomes and predictive factors for biochemical relapse following primary androgen deprivation therapy in men with bone scan negative prostate cancer. J Cancer Res Clin Oncol. 2011; 137:235–41. [PubMed: 20390426]

151. Rigaud J, Tiguert R, Le Normand L, et al. Prognostic value of bone scan in patients with metastatic prostate cancer treated initially with androgen deprivation therapy. J Urol. 2002; 168:1423–6. [PubMed: 12352409]

152. Wosnitzer B, Ghesani M. Paradoxical response of prostate cancer skeletal metastases to androgen deprivation therapy. Radiology Case Reports. 2010; 5:443.

153. Ganswindt U, Schilling D, Muller AC, et al. Distribution of prostate sentinel nodes: a SPECT-derived anatomic atlas. Int J Radiat Oncol Biol Phys. 2011; 79:1364–72. [PubMed: 20797823]

154. Zuckier LS, Finkelstein M, Kreutzer ER, et al. Technetium-99m antimony sulphide colloid lymphoscintigraphy of the prostate by direct transrectal injection. Nucl Med Commun. 1990; 11:589–96. [PubMed: 2234694]

155. Mattei A, Fuechsel FG, Bhatta Dhar N, et al. The template of the primary lymphatic landing sites of the prostate should be revisited: results of a multimodality mapping study. Eur Urol. 2008; 53:118–25. [PubMed: 17709171]

156. Warncke SH, Mattei A, Fuechsel FG, et al. Detection rate and operating time required for gamma probe-guided sentinel lymph node resection after injection of technetium-99m nanocolloid into the prostate with and without preoperative imaging. Eur Urol. 2007; 52:126–32. [PubMed: 17258385]

157. Ganswindt U, Paulsen F, Corvin S, et al. Intensity modulated radiotherapy for high risk prostate cancer based on sentinel node SPECT imaging for target volume definition. BMC Cancer. 2005; 5:91. [PubMed: 16048656]

158. Seo Y, Aparici CM, Chen CP, et al. Mapping of lymphatic drainage from the prostate using filtered 99mTc-sulfur nanocolloid and SPECT/CT. J Nucl Med. 2011; 52:1068–72. [PubMed: 21680690]

159. Minner S, Wittmer C, Graefen M, et al. High level PSMA expression is associated with early PSA recurrence in surgically treated prostate cancer. Prostate. 2011; 71:281–8. [PubMed: 20809553]

160. Slovin SF. Emerging role of immunotherapy in the management of prostate cancer. Oncology (Williston Park). 2007; 21:326–33. discussion 334, 338, 346-8. [PubMed: 17447437]

161. Ross JS, Sheehan CE, Fisher HA, et al. Correlation of primary tumor prostate-specific membrane antigen expression with disease recurrence in prostate cancer. Clin Cancer Res. 2003; 9:6357–62. [PubMed: 14695135]

162. Burger MJ, Tebay MA, Keith PA, et al. Expression analysis of delta-catenin and prostate-specific membrane antigen: their potential as diagnostic markers for prostate cancer. Int J Cancer. 2002; 100:228–37. [PubMed: 12115574]

163. Bander NH. Technology insight: monoclonal antibody imaging of prostate cancer. Nat Clin Pract Urol. 2006; 3:216–25. [PubMed: 16607370]

164. Sodee DB, Ellis RJ, Samuels MA, et al. Prostate cancer and prostate bed SPECT imaging with ProstaScint: semiquantitative correlation with prostatic biopsy results. Prostate. 1998; 37:140–8. [PubMed: 9792131]

165. Pandit-Taskar N, O'Donoghue JA, Morris MJ, et al. Antibody mass escalation study in patients with castration-resistant prostate cancer using 111In-J591: lesion detectability and dosimetric projections for 90Y radioimmunotherapy. J Nucl Med. 2008; 49:1066–74. [PubMed: 18552139]

166. Bander NH, Trabulsi EJ, Kostakoglu L, et al. Targeting metastatic prostate cancer with radiolabeled monoclonal antibody J591 to the extracellular domain of prostate specific membrane antigen. J Urol. 2003; 170:1717–21. [PubMed: 14532761]

167. Milowsky MI, Nanus DM, Kostakoglu L, et al. Phase I trial of yttrium-90-labeled anti-prostate-specific membrane antigen monoclonal antibody J591 for androgen-independent prostate cancer. J Clin Oncol. 2004; 22:2522–31. [PubMed: 15173215]

168. Morris MJ, Divgi CR, Pandit-Taskar N, et al. Pilot trial of unlabeled and indium-111-labeled anti-prostate-specific membrane antigen antibody J591 for castrate metastatic prostate cancer. Clin Cancer Res. 2005; 11:7454–61. [PubMed: 16243819]

169. Patri AK, Myc A, Beals J, et al. Synthesis and in vitro testing of J591 antibody-dendrimer conjugates for targeted prostate cancer therapy. Bioconjug Chem. 2004; 15:1174–81. [PubMed: 15546182]

170. Vallabhajosula S, Goldsmith SJ, Hamacher KA, et al. Prediction of myelotoxicity based on bone marrow radiation-absorbed dose: radioimmunotherapy studies using 90Y- and 177Lu-labeled J591 antibodies specific for prostate-specific membrane antigen. J Nucl Med. 2005; 46:850–8. [PubMed: 15872360]

171. Bander NH, Milowsky MI, Nanus DM, et al. Phase I trial of 177lutetium-labeled J591, a monoclonal antibody to prostate-specific membrane antigen, in patients with androgen-independent prostate cancer. J Clin Oncol. 2005; 23:4591–601. [PubMed: 15837970]

172. Vallabhajosula S, Goldsmith SJ, Kostakoglu L, et al. Radioimmunotherapy of prostate cancer using 90Y- and 177Lu-labeled J591 monoclonal antibodies: effect of multiple treatments on myelotoxicity. Clin Cancer Res. 2005; 11:7195s–7200s. [PubMed: 16203821]

173. Vallabhajosula S, Kuji I, Hamacher KA, et al. Pharmacokinetics and biodistribution of 111In- and 177Lu-labeled J591 antibody specific for prostate-specific membrane antigen: prediction of 90Y-J591 radiation dosimetry based on 111In or 177Lu? J Nucl Med. 2005; 46:634–41. [PubMed: 15809486]

174. Holland JP, Divilov V, Bander NH, et al. 89Zr-DFO-J591 for immunoPET of prostate-specific membrane antigen expression in vivo. J Nucl Med. 2010; 51:1293–300. [PubMed: 20660376]

175. Hillier SM, Kern AM, Maresca KP, et al. 123I-MIP-1072, a small-molecule inhibitor of prostate-specific membrane antigen, is effective at monitoring tumor response to taxane therapy. J Nucl Med. 2011; 52:1087–93. [PubMed: 21680691]

176. Ellis RJ, Sodee DB, Spirnak JP, et al. Feasibility and acute toxicities of radioimmunoguided prostate brachytherapy. Int J Radiat Oncol Biol Phys. 2000; 48:683–7. [PubMed: 11020564]

177. Ellis RJ, Zhou EH, Fu P, et al. Single photon emission computerized tomography with capromab pendetide plus computerized tomography image set co-registration independently predicts biochemical failure. J Urol. 2008; 179:1768–73. discussion 1773-4. [PubMed: 18343445]

178. Seo Y, Aparici CM, Cooperberg MR, et al. In vivo tumor grading of prostate cancer using quantitative 111In-capromab pendetide SPECT/CT. J Nucl Med. 2010; 51:31–6. [PubMed: 20008977]

179. Minamimoto R, Uemura H, Sano F, et al. The potential of FDG-PET/CT for detecting prostate cancer in patients with an elevated serum PSA level. Ann Nucl Med. 2011; 25:21–7. [PubMed: 20931305]

180. Hofer C, Laubenbacher C, Block T, et al. Fluorine-18-fluorodeoxyglucose positron emission tomography is useless for the detection of local recurrence after radical prostatectomy. Eur Urol. 1999; 36:31–5. [PubMed: 10364652]

181. Costello LC, Franklin RB. Citrate metabolism of normal and malignant prostate epithelial cells. Urology. 1997; 50:3–12. [PubMed: 9218011]

182. Ponde DE, Dence CS, Oyama N, et al. 18F-fluoroacetate: a potential acetate analog for prostate tumor imaging--in vivo evaluation of 18F-fluoroacetate versus 11C-acetate. J Nucl Med. 2007; 48:420–8. [PubMed: 17332620]

183. Matthies A, Ezziddin S, Ulrich EM, et al. Imaging of prostate cancer metastases with 18F-fluoroacetate using PET/CT. Eur J Nucl Med Mol Imaging. 2004; 31:797. [PubMed: 14985862]

184. Bauman G, Belhocine T, Kovacs M, et al. (18)F-fluorocholine for prostate cancer imaging: a systematic review of the literature. Prostate Cancer Prostatic Dis. 2012; 15:45–55. [PubMed: 21844889]

185. Beheshti M, Vali R, Langsteger W. [18F]fluorocholine PET/CT in the assessment of bone metastases in prostate cancer. Eur J Nucl Med Mol Imaging. 2007; 34:1316–7. author reply 1318-9. [PubMed: 17476505]

186. Cimitan M, Bortolus R, Morassut S, et al. [18F]fluorocholine PET/CT imaging for the detection of recurrent prostate cancer at PSA relapse: experience in 100 consecutive patients. Eur J Nucl Med Mol Imaging. 2006; 33:1387–98. [PubMed: 16865395]

187. Kwee SA, Wei H, Sesterhenn I, et al. Localization of primary prostate cancer with dual-phase 18F-fluorocholine PET. J Nucl Med. 2006; 47:262–9. [PubMed: 16455632]

188. Heinisch M, Dirisamer A, Loidl W, et al. Positron emission tomography/computed tomography with F-18-fluorocholine for restaging of prostate cancer patients: meaningful at PSA < 5 ng/ml? Mol Imaging Biol. 2006; 8:43–8. [PubMed: 16315004]

189. Schmid DT, John H, Zweifel R, et al. Fluorocholine PET/CT in patients with prostate cancer: initial experience. Radiology. 2005; 235:623–8. [PubMed: 15858102]

190. Kwee SA, Coel MN, Lim J, et al. Prostate cancer localization with 18fluorine fluorocholine positron emission tomography. J Urol. 2005; 173:252–5. [PubMed: 15592091]

191. Wurschmidt F, Petersen C, Wahl A, et al. [18F]fluoroethylcholine-PET/CT imaging for radiation treatment planning of recurrent and primary prostate cancer with dose escalation to PET/CT-positive lymph nodes. Radiat Oncol. 2011; 6:44. [PubMed: 21529377]

192. Steuber T, Schlomm T, Heinzer H, et al. [F(18)]-fluoroethylcholine combined in-line PET-CT scan for detection of lymph-node metastasis in high risk prostate cancer patients prior to radical prostatectomy: Preliminary results from a prospective histology-based study. Eur J Cancer. 2010; 46:449–55. [PubMed: 19969447]

193. Pascali G, D'Antonio L, Bovone P, et al. Optimization of automated large-scale production of [(18)F]fluoroethylcholine for PET prostate cancer imaging. Nucl Med Biol. 2009; 36:569–74. [PubMed: 19520298]

194. Zuhayra M, Alfteimi A, Papp L, et al. Simplified fast and high yielding automated synthesis of [18F]fluoroethylcholine for prostate cancer imaging. Bioorg Med Chem. 2008; 16:9121–6. [PubMed: 18819809]

195. Hara T, Kosaka N, Kishi H. Development of (18)F-fluoroethylcholine for cancer imaging with PET: synthesis, biochemistry, and prostate cancer imaging. J Nucl Med. 2002; 43:187–99. [PubMed: 11850483]

196. Oyama N, Akino H, Suzuki Y, et al. FDG PET for evaluating the change of glucose metabolism in prostate cancer after androgen ablation. Nucl Med Commun. 2001; 22:963–9. [PubMed: 11505204]

197. Baronzio G, Gramaglia A, Fiorentini G. Review. Current role and future perspectives of hyperthermia for prostate cancer treatment. In Vivo. 2009; 23:143–6. [PubMed: 19368139]

198. Picchio M, Giovannini E, Crivellaro C, et al. Clinical evidence on PET/CT for radiation therapy planning in prostate cancer. Radiother Oncol. 2010; 96:347–50. [PubMed: 20708811]

199. Winter A, Uphoff J, Henke RP, et al. First results of [11C]choline PET/CT-guided secondary lymph node surgery in patients with PSA failure and single lymph node recurrence after radical retropubic prostatectomy. Urol Int. 2010; 84:418–23. [PubMed: 20299773]

200. Winter A, Uphoff J, Henke RP, et al. Complete PSA Remission without Adjuvant Therapy after Secondary Lymph Node Surgery in Selected Patients with Biochemical Relapse after Radical Prostatectomy and Pelvic Lymph Node Dissection. Adv Urol. 2012; 2012:609612. [PubMed: 21754926]

201. Yu EY, Muzi M, Hackenbracht JA, et al. C11-acetate and F-18 FDG PET for men with prostate cancer bone metastases: relative findings and response to therapy. Clin Nucl Med. 2011; 36:192–8. [PubMed: 21285676]

202. Seppala J, Seppanen M, Arponen E, et al. Carbon-11 acetate PET/CT based dose escalated IMRT in prostate cancer. Radiother Oncol. 2009; 93:234–40. [PubMed: 19766336]

203. Breeuwsma AJ, Pruim J, Jongen MM, et al. In vivo uptake of [11C]choline does not correlate with cell proliferation in human prostate cancer. Eur J Nucl Med Mol Imaging. 2005; 32:668–73. [PubMed: 15765234]

204. Farsad M, Schiavina R, Castellucci P, et al. Detection and localization of prostate cancer: correlation of (11)C-choline PET/CT with histopathologic step-section analysis. J Nucl Med. 2005; 46:1642–9. [PubMed: 16204714]

205. Beattie BJ, Smith-Jones PM, Jhanwar YS, et al. Pharmacokinetic assessment of the uptake of 16beta-18F-fluoro-5alpha-dihydrotestosterone (FDHT) in prostate tumors as measured by PET. J Nucl Med. 2010; 51:183–92. [PubMed: 20080885]

206. Apolo AB, Pandit-Taskar N, Morris MJ. Novel tracers and their development for the imaging of metastatic prostate cancer. J Nucl Med. 2008; 49:2031–41. [PubMed: 18997047]

207. He J, Wang Y, Feng J, et al. Targeting prostate cancer cells in vivo using a rapidly internalizing novel human single-chain antibody fragment. J Nucl Med. 2010; 51:427–32. [PubMed: 20150269]

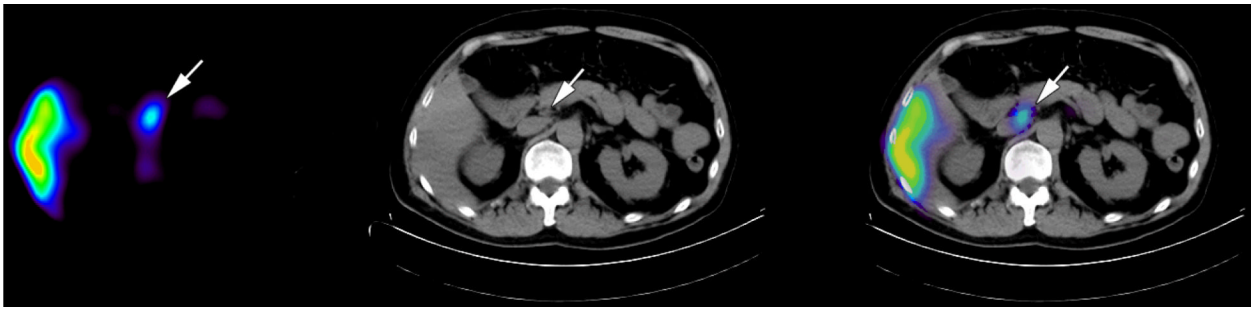

Figure 1.

1.5 cm × 0.7 cm peripancreatic lymph node uptake of ^{111}In-capromab pendetide visualized by SPECT combined with 16-slice multidetector CT (Precedence, Philips Healthcare) scanner. Transverse images of SPECT alone (left); CT alone (middle); and SPECT/CT fusion (right). Arrows indicate where the ^{111}In-capromab pendetide uptake is in relation to its anatomical location from SPECT, CT, and SPECT/CT images. Reprinted with permission under the “Creative Commons Attribution Noncommercial License”.[48]

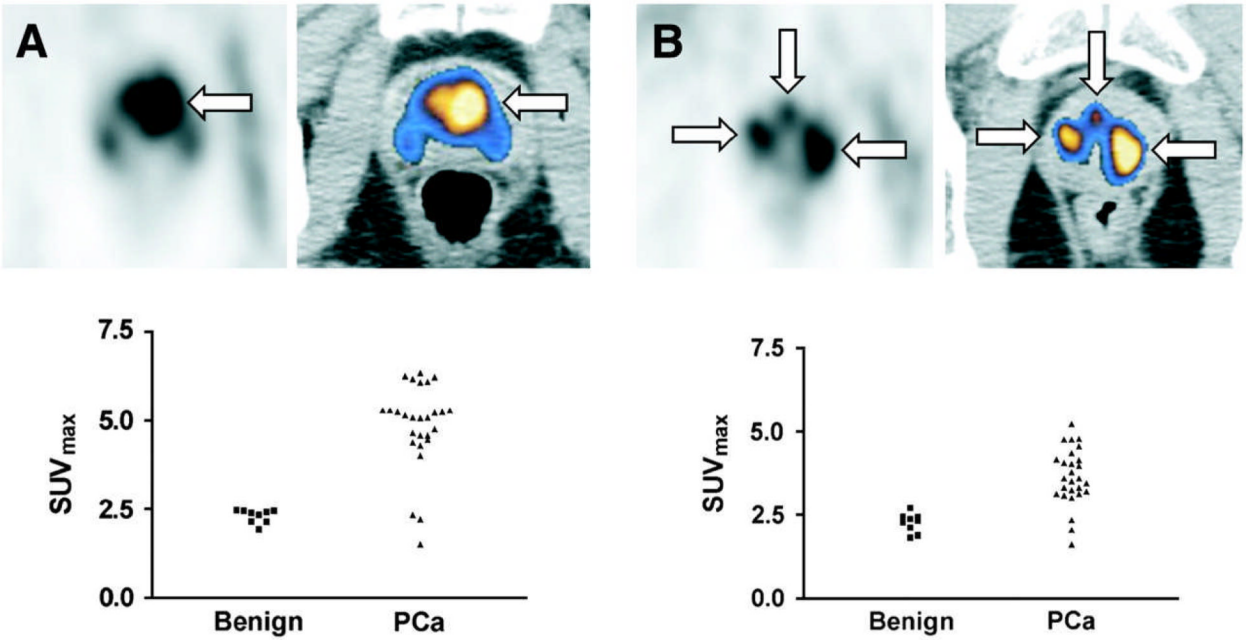

Figure 2.
^{11}C-choline PET/CT showing focal (A) and multifocal (B) lesion distribution of prostate cancer within the gland (arrows). The scatter plots show the maximum standardized uptake values (SUV_{max}) for each scan in 36 segments within the gland, which were divided by 6 peripheral and 6 central segments, totaling 36 segments. Reprinted with permission.[78]

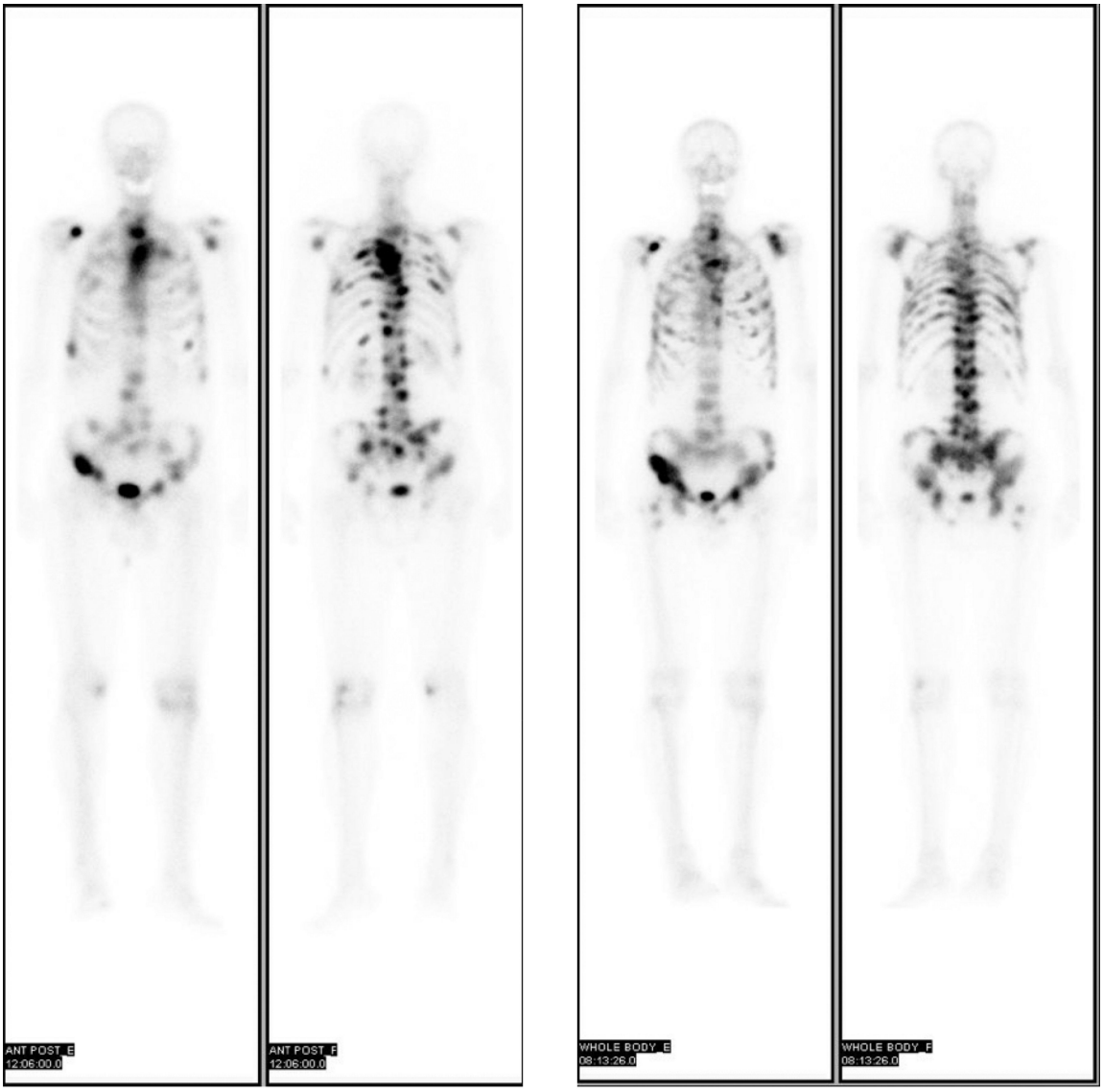

Figure 3.
Pretherapy (left) and posttherapy (right) ^{99m}Tc-MDP anterior-posterior bone scans showing geographic distributions of skeletal metastases. The response to the androgen deprivation therapy for the patient with metastatic prostate cancer is depicted by bone scan, and the different geographical locations of bone lesions show different responses to the therapy. Reprinted with permission under the “Creative Commons Attribution-NonCommercial-NoDerivs”.[152]

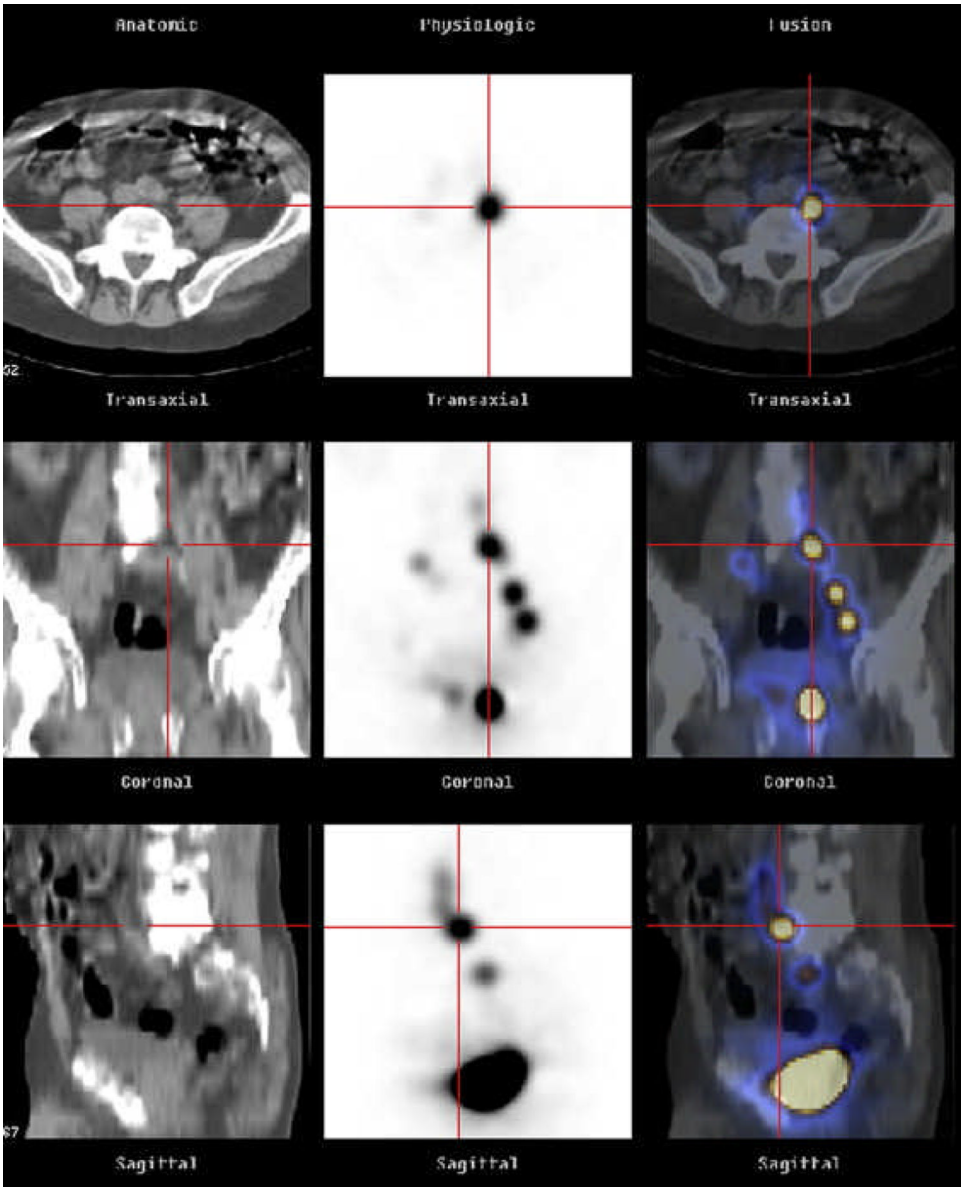

Figure 4.
SPECT/CT example of ^{99m}Tc-nanocolloid injected to the prostate gland, showing three sentinel lymph nodes (iliac left) identified by this imaging technique. Reprinted with permission.[153]

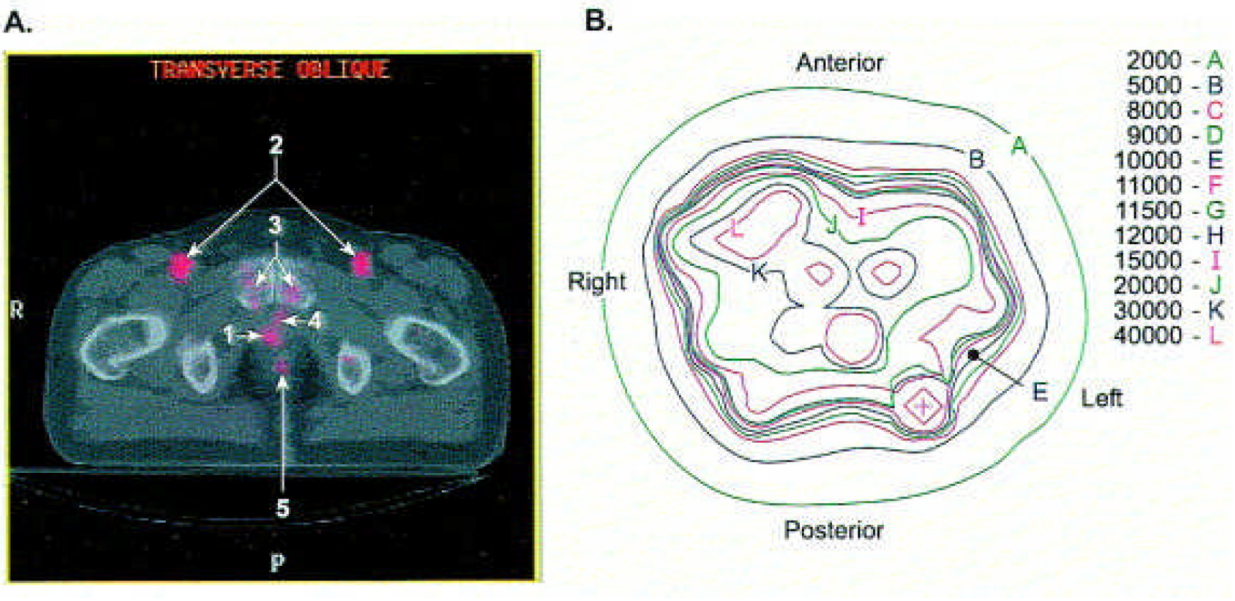

Figure 5.

Transverse view (left) of ^{111}In-capromab pendetide SPECT fused with CT from a patient undergoing ultrasound-guided brachytherapy using Pd-103 seeds. Additional seeds were used during implantation for the regions identified by ^{111}In-capromab pendetide SPECT/CT, showing the feasibility of dose escalation based on the imaging data. The dose distribution map (right) of the brachytherapy shows the isodose map at 9mm superior to the midplane of the seed-implanted volume. Reprinted with permission.[176]

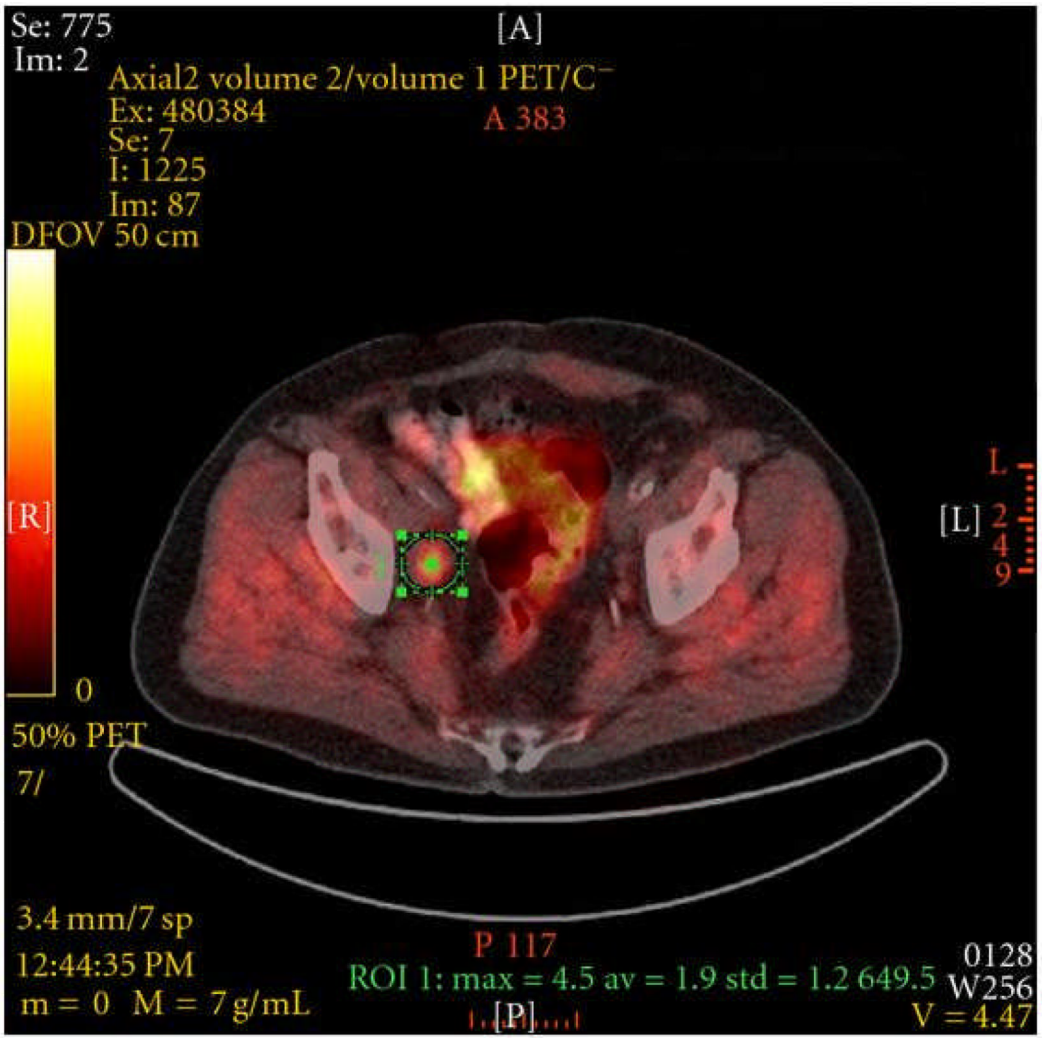

Figure 6.
Transverse view of 11C-choline PET/CT showing a single lymph node metastasis of prostate cancer in the right iliac region. The metastatic cancer was confirmed by histopathology after resection. Reprinted with permission under the “Created Commons Attribution License”.[200]

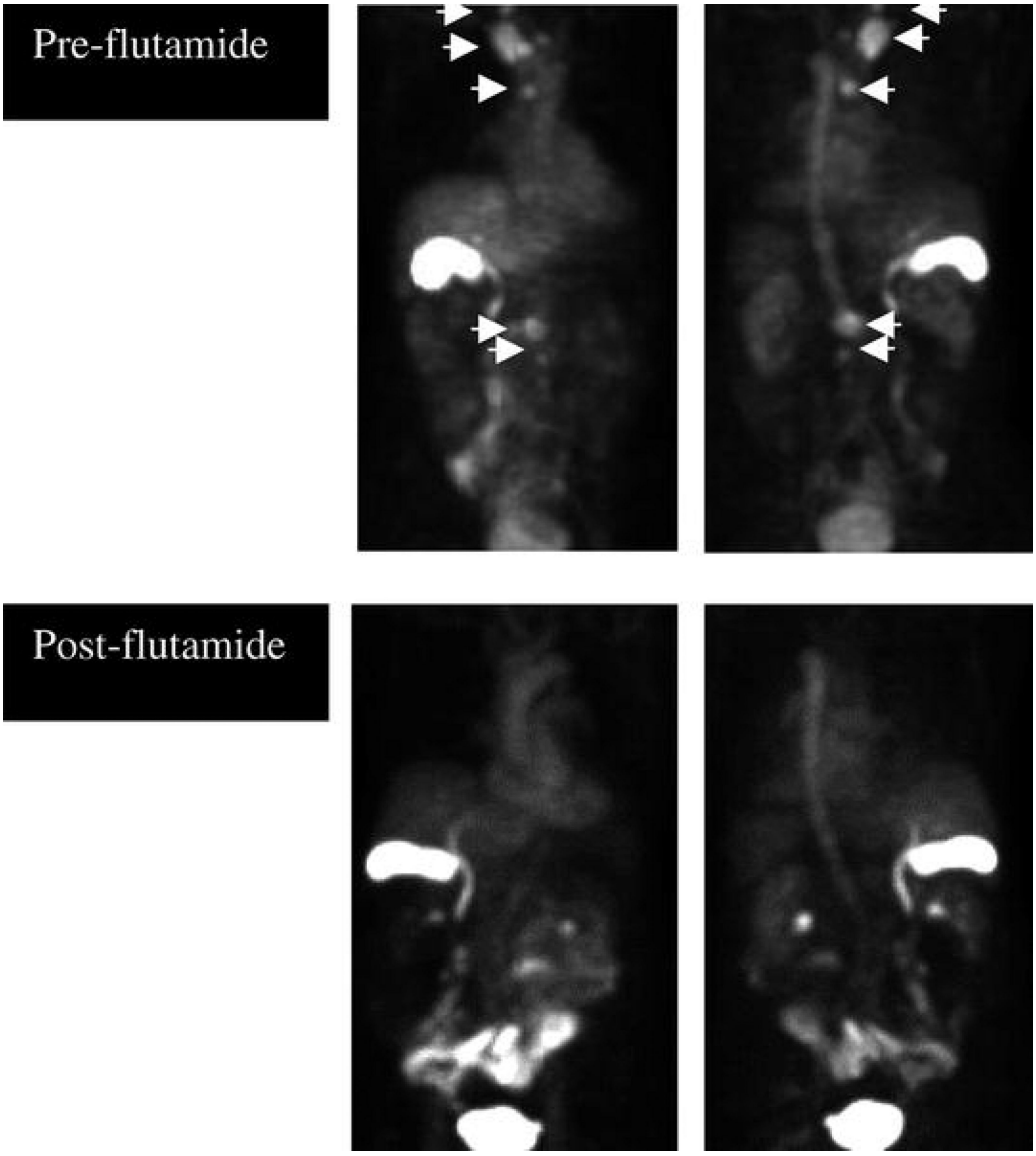

Figure 7.
Maximum-pixel-intensity reprojection images of ^{18}F-FDHT before and after flutamide (androgen receptor antagonist) treatment. Images show anterior (left) and posterior (right) views, and pretherapy (upper row) and posttherapy (lower row) views. Arrows indicate the lymph nodes that had strong ^{18}F-FDHT uptake before flutamide therapy. After the therapy, the ^{18}F-FDHT uptake disappeared in these lymph nodes. Reprinted with permission.[147]